The magneto optical system at Risø

Larsen, Britt Hvolbæk

Publication date:
2001

Document Version
Publisher's PDF, also known as Version of record

Risø-R-1262(EN)

The Magneto Optical System at Risø

Britt Hvolbæk Larsen

Risø National Laboratory, Roskilde
April 2001

Abstract The new magneto optical system at Risø is presented in details. Results measured on the system is shown. Image correction and magnetic field to current density conversion is described.

ISBN 87-550-2867-5
ISBN 87-550-2868-3(internet)
ISSN 0106-2840

Print: Danka Services International A/S, 2001

Contents

Preface

The idea of building a magneto optical system in the Superconductivity group at the Condensed Matter Physics and Chemistry Department was conceived by Niels Hessel Andersen, who also secured funding to build the system from STVF and EFP as well as design and purchase of the system.

A large credit and thank go to our technician Steen Nielsen, who was always there to help with problems large and small when building the magneto optical system. His insisting on making the correct and lasting solution taught me much about good craftmanship. Any item that seems less than well designed is probably due to my overruling of his suggestions. We thank Torben Kjær for designing and building the very useful translation stage for the microscope. We also thank Per Skaarup for programming the Tascom extensions we needed.

Paragraph 1.1 is based on the application for the EFP and STVF written by Niels Hessel Andersen and Thomas Frello. Paragraph 1.2 relies heavily on the Ph.D. theses of Petriina Paturi [4] and Thomas Frello [5]. I am grateful to Birgitte Abery Jakobsen and Asger Abrahamsen for the many useful suggestions to the measurements and this report. I thank Frederik C. Krebs for suggesting the gold plating method described in appendix B.2.

The method described for background correction of the pictures was suggested to us by Kari Nilsson and Petriina Paturi both from University of Turku, Finland. We are grateful to Petriina for allowing us to use the program developed by her for the field to critical current inversion of the MO images.

Appendix B.11 on sample polishing and part of appendix B6 on MO indicator cleaning is based on a report by M. Koblischka and chapter 3.7 is based on his contributions to the annual Risø report.

1 BACKGROUND AND THEORY

1.1 Motivation

In 1999 the Condensed Matter Physics and Chemistry Department received grants from EFP and STVF to build a magneto optic system. The aim was to establish a technique that maps the magnetic flux distribution with a spatial resolution of a few micrometer and a time resolution of about 50 ms. The overall purpose was to identify current paths with low critical current and improve the flux pinning in applied superconducting materials.

In the development of high temperature superconductors for application purposes, a number of unsolved problems exists, especially in applications where the superconductors ability to carry high currents is used to induce strong magnetic field, but also to some extent in high power transmission cables, where the self field should not decrease the superconducting properties. The problems arise from the ceramic character of the material, its anisotropic crystal structure and generally from the fact that superconductivity is suppressed by magnetic fields. The ceramic character and anisotropic electrical properties mean that the crystallites must be well aligned and compacted to obtain good electrical contact. The grain boundaries in the ceramic will often have significantly lower critical current than the crystallites themselves, and in a magnetic field the reduction is even more pronounced. Therefore, even a weak self field can significantly reduce the critical current. Non-superconducting phases and cracks will of course also reduce the superconducting properties.
The fundamental reason for the supression of superconductivity by magnetic fields is well known and directly related to the way the superconductor forms electron pairs. It is also well known that superconductors oppose the effect of the magnetic fields by setting up superconducting - and thereby loss-free - currents, which either exclude the magnetic field from the bulk of the superconductor or isolate the magnetic field in flux lines with a fix amount of magnetic flux. The magnetic fluxlines interacts with the currents and move in a loss giving way, if they are not pinned. The structure of the flux lines and the properties of the pinning determine how much current a superconductor can carry without loss. If the flux lines form a rigid flux line lattices it takes little energy to pin them, but if the flux lines can move independently like a liquid, they need to be

pinned individually. Defects, grain boundaries and non-superconducting impurities act as pinning centers, but at the same time act to decrease the superconductivity.
If an external magnetic field is applied to a superconductor, the flux lines will penetrate into a layer of the surface sufficiently thick that the shielding currents balance the external field. If the magnetic field is increased it will penetrate further into the superconductor. The flux penetration in the grains is a measure of how the critical current depends on the magnetic field. If the flux pinning is small, the flux lines can move by e.g. thermal excitation or electrical current through the superconductor. The flux penetration along the grain boundaries reflects the poor superconducting connection between the grains. Using time resolved studies of the flux penetration it would be possible to study both the grains and the grain boundaries. Thereby weak current paths in the superconducting materials can be identified.

1.2 Background

Magneto-optical microscopy is based on the Faraday rotation of linearly polarized light in an indicator film placed on top of a sample [1,2]. The rotation angle, θ, of the polarized light in the magneto-optically active material is:

$$\theta = VlH$$

where l is the optical path length in the indicator film, H is the magnetic field perpendicular to the indicator and the Verdet constant, V, is material specific. The rotation angle of the incident light will vary spatially depending on the magnetic field in the point where the light is reflected from. Thus spatial information of the perpendicular magnetic field on the surface of the sample can be obtained. The field shielding response of a superconductor gives a strong spatial modulation of the total field just above the superconductor. This can be imaged by magneto optical microscopy.
The magneto optical layer in our films is ferrimagnetic Bismuth doped yttrium-ion garnets (Bi:YIG). The magnetic moments order in the plane of the garnet film. An applied magnetic field tilts the spins out of the plane. This gives a different propagation velocity for right- and left handed circular polarized light. As a consequence, linearly polarized light will be turned an angle θ.

The magnetic field from a current loop along its rotation axis is:

$$H_z = \frac{nIa^2}{2(z^2 + a^2)^{3/2}}$$

where a is the radius of the current loop, I is the current running in it, n is the number of turns, and z is the distance along the perpendicular axis.

This decreases as $1/z^2$. From the expression it is seen that the smaller the current loop, the faster the field falls off.
For a one-dimensional structure like a wire the field is:

$$H = \frac{I}{2\pi r}$$

where I is the current in the wire and r is the perpendicular distance to the wire. If the current is in the plane, the field falls off as 1/z in a direction perpendicular to the plane.
The consequence of these consideration is that if a current loop is very small compared to the distance between the MO film and the current loop, the magnetic field can decrease so quickly, that no signal is seen in the MO indicator film. Therefore, it is essential to have the MO indicator film very close to the sample if good spatial resolution is needed. In the recent measurement of flux lines in high-T_c superconductors at the University of Oslo, the MO indictor film was grown directly on top of the sample to minimize this distance [3].

In a type II superconductor complete shielding of an external magnetic field takes place only below H_{c1}, the first critical field. Here the superconductor is in the Meissner state. This is typically a small field (below 10 mT). Between the first critical field and the second critical field, H_{c2}, the superconductor is in a mixed state where magnetic flux has penetrated the superconductor, but superconductivity persists. The second critical field H_{c2} may be several hundreds of teslas in high-T_c materials [4].
In the mixed state shielding currents around the penetrated flux lines are present in the superconductor. Several models have been suggested to describe the distribution of these flux lines. The simplest model is the Bean model. It assumes that a superconductor in an applied magnetic field will set up shielding currents along the edges. The current density of the current along the edges will be the critical current density, j_c, which is assumed to be constant. This current density will extend into the sample sufficiently deep to counteract the applied magnetic field and keep the total magnetic field zero in the center of the superconductor. The magnetic field will fall of linearly over the zone where there is a constant current density as seen in figure 1.1. The Bean model is widely used since the constant value of j_c simplifies calculations considerably. [5]

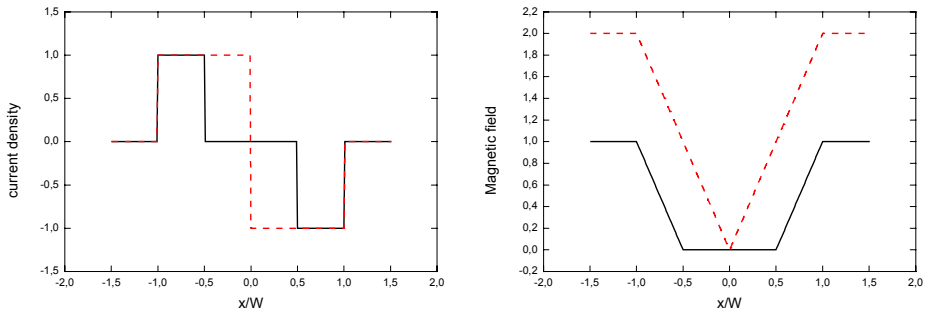

Figure 1.1: The current density and magnetic field profile of a sample with width w for two values of the applied magnetic field.

The Anderson-Kim model is an extension of the Bean model [4]. It includes the field dependence of the critical current and assumes a dependence given as $J_c=J_c(0)/(1+B/B_0)$. This leads to a parabolic variation of the internal magnetic field. Several variations of the Anderson-Kim model exists with different dependency of the critical current density of the magnetic field.
The field profiles of the Bean and Kim-Anderson models are strictly speaking only valid for a long sample in a parallel magnetic field. Since most magneto-optical microscopy takes place on thin samples with the magnetic field applied perpendicular to the surface, this case must be further investigated. Mathematically, getting from a geometry where the sample is infinitely long in the dimension parallel to the magnetic field to a geometry where the dimension parallel to the magnetic field is smaller than the width of the sample is obtained by a conformal mapping [6]. This changes the magnetic field profile even if a Bean model is used for the current density as seen in figure 1.2.

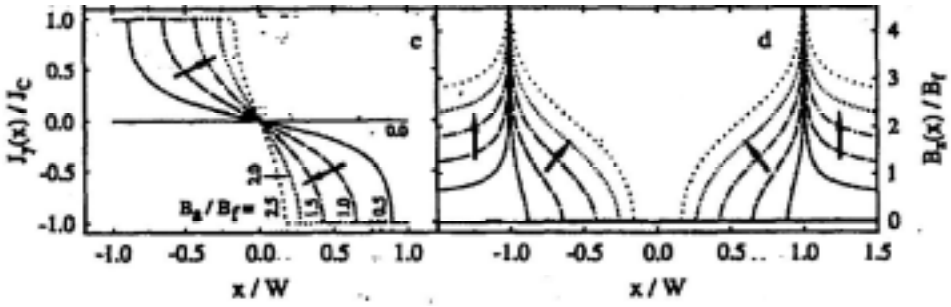

Figure 1.2: Magnetic field profile over thin film from [6]

If the current density depends on the magnetic field, the field profiles can only be calculated using numerical methods [4,7,8]

The MO image gives the distribution of the *z*-component of the magnetic field. The relation between magnetic field and current density is given by Biot and Savart's law:

$$\vec{H}(\vec{r}) = \frac{1}{4\pi}\int_V \vec{j}(\vec{s}) \times \frac{\vec{r}-\vec{s}}{\left|\vec{r}-\vec{s}\right|^3} d^3s$$

In general, it is not posssible to convert a magnetic field image into a unique current density image. And here we even only have one component of the magnetic field. The first constraint introduced is that the current is only flowing in the plane. This 'flat sample' assumption used by all the suggested methods for the inversion from magnetic field to current density. Two classes of methods have been suggested [9-15]. One uses a Fourier transform with spatial filtering for the deconvolution of the current density [9,10]. In the other method, introduced by Wijngaarden [11], the matrix equation is solved after discretization of Biot-Savart's law. The obtained dipole density is then inverted into the current density. This last method is implemented in the program developed by Petriina Paturi from the University of Turku, Finland [4].

Figure 1.3 shows the general geometry, that is solved by the Wijngaarden method. The main steps in the calculation is now described: The sample is assumed flat with a uniform current density along the *z*-direction. When is assumed that the current flows only in the *x* and *y* directions, the current density can be linked to a scalar field as follows:

$$\vec{j}(\vec{s}) = \nabla_{\vec{s}} \times (g(\vec{s})\hat{z})'$$

Biot and Savart's law is then rewritten as:

$$\vec{H}(\vec{r}) = \frac{1}{4\pi}\int_V g(\vec{s})\frac{3\hat{r}(\vec{z}\cdot\hat{z})}{\left|\vec{r}-\vec{s}\right|^3}d^3s$$

where $\hat{n} = ((\vec{r}-\vec{s})/\left|\vec{r}-\vec{s}\right|)$. Now write the vectors $\vec{s}$ and $\vec{r}$ as a component in the plane and a normal component as seen in figure 1.3. The MO image is already discretized, and the pixels in the image can be identified with the indices (*i, j)*. A similar discretization of the sample surface can be given by *(k, l)* pairs. The pixels are assumed to be squares with size *a*. The equation for the measured *z*-component of the magnetic field then becomes:

$$H_z(i,j,h) = \frac{1}{4\pi}\sum_{k,l} g(k,l)\int_{k-½}^{k+½}\int_{l-½}^{l+½}\int_0^d \frac{2(d+\zeta)^2 - a^2(\xi-i)^2 - a^2(\eta-j)^2}{\left[(d+\zeta)^2 + a^2(\xi-i)^2 + a^2(\eta-j)^2\right]^{5/2}} d\zeta d\eta d\xi$$

This can be written as:

$$H_z(i,j,h) = \frac{1}{4\pi}\sum_{k,l} M(i,j,k,l)g(k,l)$$

By inverting the matrix *M* the scalar field *g(k, l)* is obtained, and from this the current density can be found. More details of the method is found in Wijngaarden's paper [11].

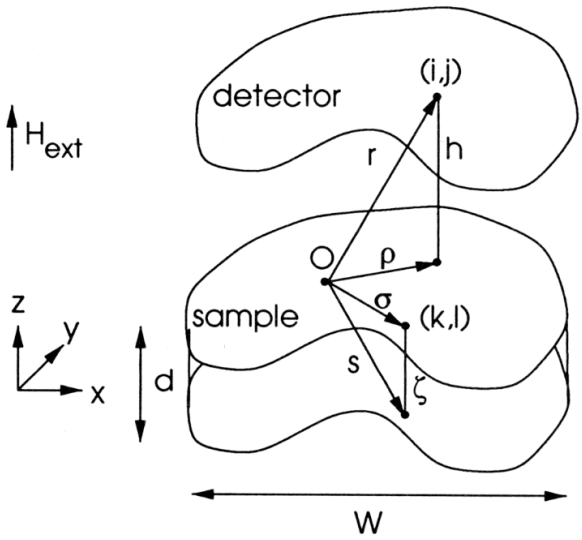

Figure 1.3: The geometry used in Wijngaarden's inversion method.

2 MAGNETO OPTICAL SYSTEM

2.1 Introduction

A magneto-optical (MO) system has been established in the Department during 1999-2000. This technique enables spatially local and time resolved measurements of the magnetic field distribution over a flat sample.
A schematic diagram of the MO system and a photograph of the setup are shown in figure 2.1. The setup consists of a cryogenic system, an imaging system, and the magnetic field coil and magneto-optical films. Monochromatic light is polarized and shined onto an MO indicator film, which due to the Faraday effect rotates the polarization of the light proportionally to the local magnetic field. The reflected light meets a polarization filter with is rotated 90° with respect to the first polarizer. In this way, the magnetic field distribution at the surface of the sample positioned below the indicator film is seen. The cryostat can be operated between 4 K and 300 K and the magnetic field distribution can be determined with a spatial resolution of 2 μm and a time resolution of 20ms.
In this chapter is a detailed description of the system. Some technical aspects are referred to appendices.

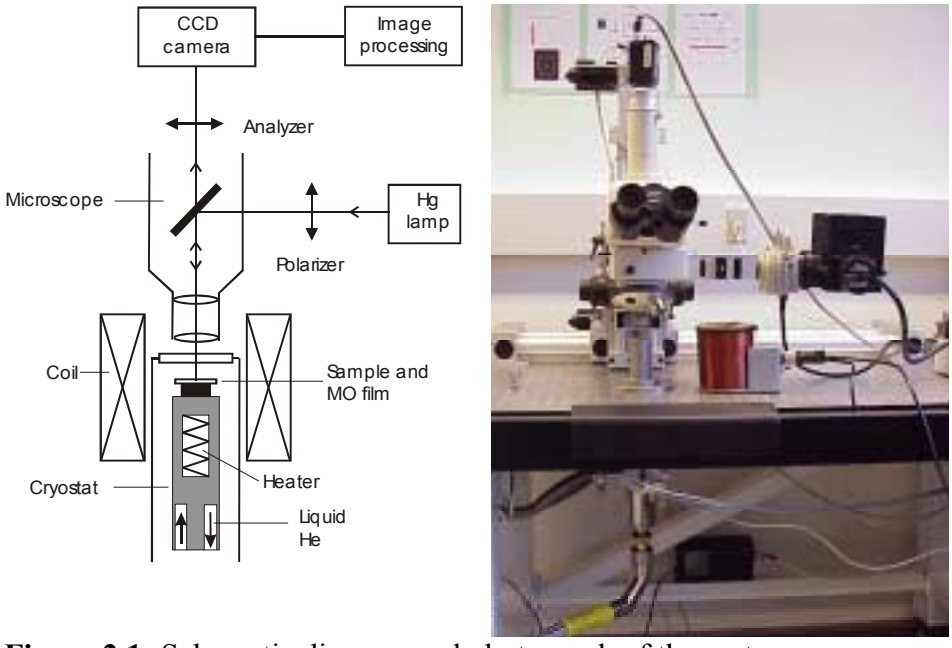

Figure 2.1: Schematic diagram and photograph of the system.

2.2 Cryogenic system

The cryogenic system consists of an open flow cryostat, two pumps, a temperature controller and a transfer line connecting the cryostat to a dewar. The principle of an open flow cryostat is to have a dewar of liquid He with elevated pressure over the liquid. The pressure forces a flow of liquid He through the cryostat. When the liquid He reaches the cryostat it evaporates and the gas is led away. The flow of liquid He determines the cooling power, and no bath of liquid He is present in the cryostat.
The cryostat is an APD cryogenics model LT-3B-110 open cycle system [16]. It operates equally well with liquid Helium or liquid Nitrogen. A picture of the cryostat as it arrived from the factory is seen in figure 2.2. The cryostat is mounted through a hole in a vibration-damped table and fitted with a vacuum shield, which is fixed to the table. The cryostat is positioned with the cold finger pointing upwards and the transfer line connects from below the table. The vacuum shield has a glass window at the top with an O-ring to the vacuum shield. This allows optical access to the cold finger. Figure 2.3 shows a closeup of the cryostat mounted in the optical table.

Figure 2.2: Flow cryostat as it arrived from the factory. The heat shield for the cold finger is lying next to it. The white cable is for the heater in the cryostat head.

Figure 2.3: Closeup of cryostat mounted upside down in the optical table.

Liquid He flows to the cryostat through a flexible Z-shaped 10-foot (3 m) long transfer line. One end of the transfer line is equipped with a long bayonet and a valve for evacuating the transfer line vacuum shield as seen in figure 2.4(right). The transfer line vacuum shield should be pumped to 10^{-4} torr. The long bayonet is inserted into a pipe with a NW50 flange. The NW50 flange fits onto the liquid He dewar and the long bayonet is inserted into the dewar.
Above the NW50 flange are four inlets. On one is a pressure gauge that measures the pressure in the dewar in kg/cm^2 (1 kg/cm^2 = 10^5 Pa = 1 bar). The second inlet is for connecting a pressurized gas container. The third

is a 5 psi (1 psi = 6894 Pa = 0.069 kg/cm^2) relief valve. 5 psi is the recommended pressure in the dewar during cool down and operation. On the last inlet is a 2.5 psi relief valve which is closed off. A pressure of 2.5 psi in the dewar is recommended by the manufactures for low He consumption, but due to our modifications, low temperatures cannot be maintained at this dewar pressure.
The other end of the transfer line is inserted into the cryostat and has a short bayonet with a needle valve as seen in figure 2.4(left). At the top of the bayonet is a large nut. The number of turns this fine threaded nut is turned determines the opening of the needle valve at the tip of the short bayonet. The tip of the short bayonet is in contact with the cold finger, so the cooling power of the liquid He is applied to the cold finger.

Figure 2.4: Left: the short bayonet that is inserted into the cryostat. The large brass nut is seen. Right: the long bayonet with the NW50 flange and the different inlets

After the liquid He evaporates as it exits the transfer line close to the cold finger, the gas is led away along two paths. One is through the cryostat and out of the He exhaust port on the side of the cryostat. The other is through the transfer line in a concentric space, which encloses the liquid He line. Along with the vacuum in the transfer line this return flow helps to keep the transfer line cold. The flow in these two outlets is monitored by two flowmeters. By opening or closing the flow in these, the flow of liquid He, and thereby cooling power, can be controlled.
The cryostat is equipped with a vent gas heater close to where the transfer line is inserted. Here, the cryostat is in direct thermal contact with the outer part of the transfer line where the return He gas flows. The heater ensures that the outside of the cryostat does not ice as a consequence of this. The heater is 100 W and is powered from a 115 V ac-transformer through the white cable with the american connector seen in figure 2.2. A bi-metal switch integrated with the heater keeps the temperature of this end of the cryostat between 115-125° Fahrenheit (46-52°C).

The vacuum space around the cryostat ensures thermal insulation from room temperature. A combined membrane pump and turbo pump (Varian Turbo-DRY 70) is connected to the cryostat to provide this. For operation of the cryostat, the vacuum should be below 10^{-5} mbar. But cooling down can begin as soon as the vacuum pump is started, since it takes approximately 30 min before the transfer line is cold and liquid He reaches the cryostat. This is amble time for the pump to reach 10^{-5} mbar. The flowmeters reads approximately 10-20 mm when just gas is reaching the cryostat. When liquid He is reaching the cryostat; the flowmeters reads approximately 50 mm.

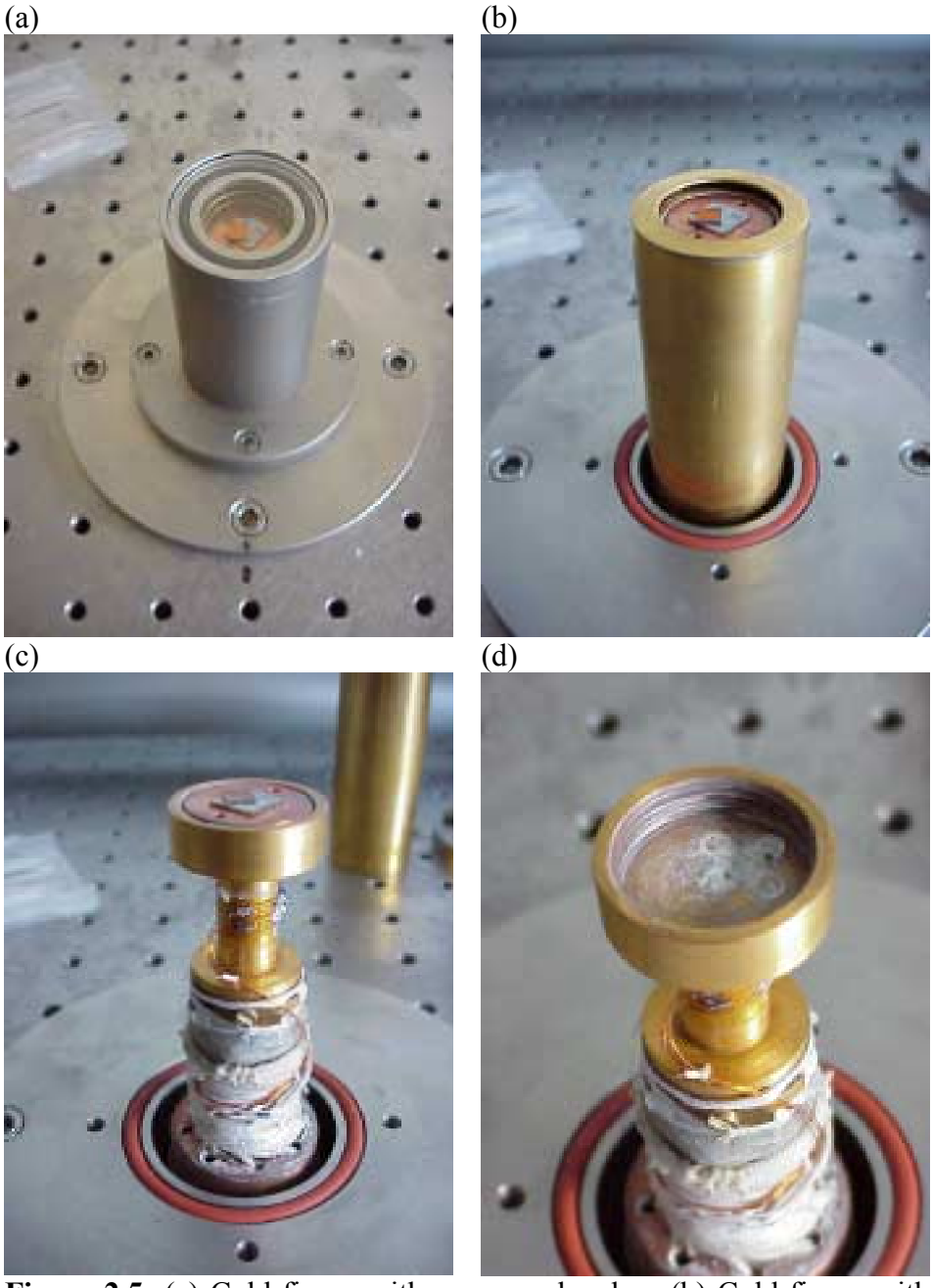

Figure 2.5: (a) Cold finger with vacuum chamber. (b) Cold finger with heat shield. (c) Cold finger with sample mount and copper disc with sample and MO indicator. (d) Sample mount with copper disc removed.

The cold finger is enclosed in a vacuum chamber that is fixed onto the optical table. This is seen in figure 2.5(a). Between the walls of the vacuum chamber and the cold finger is a heat shield, which connects to the cryostat at the base of the cold finger. We have modified this heat shield with a hole in the top to give optical access to the cold finger. Furthermore, it has been gold plated to avoid corrosion. A corroded surface on the heat shield would decrease its radiation shielding effect. The heat shield is seen in figure 2.5(b).
A sample mount has been made from OFC (oxygen free copper). It was annealed after the machining to ensure good thermal conductance and then gold plated (see appendix B2 for details). The sample mount is semi-permanently mounted on the cold finger. The gold plated sample mount is seen in figure 2.5(c). Just below the sample mount is a heater, which has been soldered onto the cold finger from the factory. It is a 20 W, 30 V heater. Figure 2.5(c) also shows the wires for the two thermometers. They are wound around the cold finger several times to prevent heating through the wires.
The sample and MO film are placed on a copper disc, which can be screwed into the sample mount from the top. Figure 2.5(d) shows the sample mount with the copper disc removed. To ensure good thermal contact to the copper disc a small amount of white thermal paste is applied to the bottom of the copper disc before it is screwed into the sample mount.

Figure 2.6: Three different copper discs for mounting samples. The lower left a flat disc with a $YBa_2Cu_3O_x$ thin film mounted. The lower right is a $Bi_2Sr_2Ca_2Cu_3O_x$ tape mounted in cross section. The upper right is a disc with a grove for a $Bi_2Sr_2Ca_2Cu_3O_x$ tape. To the upper left is the tool for screwing the copper disc into the sample mount.

Several different copper discs exist and some of them are seen in figure 2.6. The sample should be glued to the copper disc to ensure good thermal contact. A glue named conducting carbon cement (CCC) is usually used. CCC can be dissolved in acetone or toluen. The sample surface

should be flat. The MO indicator film must be placed without using glue to avoid damaging the film. (see also appendix B11).
There are two thermometers mounted. One is on the cryostat cold finger just below the sample mount. It is used as a control thermometer for the feedback loop to the heater. The other is placed in the sample mount, just below the sample disc as seen in figure 2.5(d). The thermometers are calibrated DT-421-HR Lakehore Si-diodes [22]. They are chosen because they are small and non-magnetic. To protect the leads of these fragile thermometers, they are mounted on a sapphire plate and then mounted in the cryostat (see appendix B7).
The thermometers and the heater at the cold finger are connected to a RISØ temperature controller [17]. The temperature controller is initialized from the computer program Tascom [18]. From the initialization file, the calibration table for each of the thermometers is read, it is determined which thermometer is controlling the heater output, and the PID parameters are given as a function of temperature. More about the temperature controller and Tascom can be found in appendices B8 and B9.
From the factory the cryostat has a base temperature of 2 K. Due to the modifications giving optical access to the cold finger, the base temperature of our system is about 4 K. To reach the base temperature of the cryostat we need to pump on the Helium. The needle valve in the short bayonet of the transfer line is closed down to about 2 turns (where normal operation is about 4 turns). Then the He pump is connected to the gas outlet of the cryostat. Pumping on the gas outlet decreases the pressure over the liquid Helium as it enters the cryostat, thus lowering its boiling temperature.

2.3 Imaging system

The imaging system consists of an optical microscope, a CCD camera, a framegrabber card and software to record the images. A photograph of the microscope and the CCD camera is seen in figure 2.7.

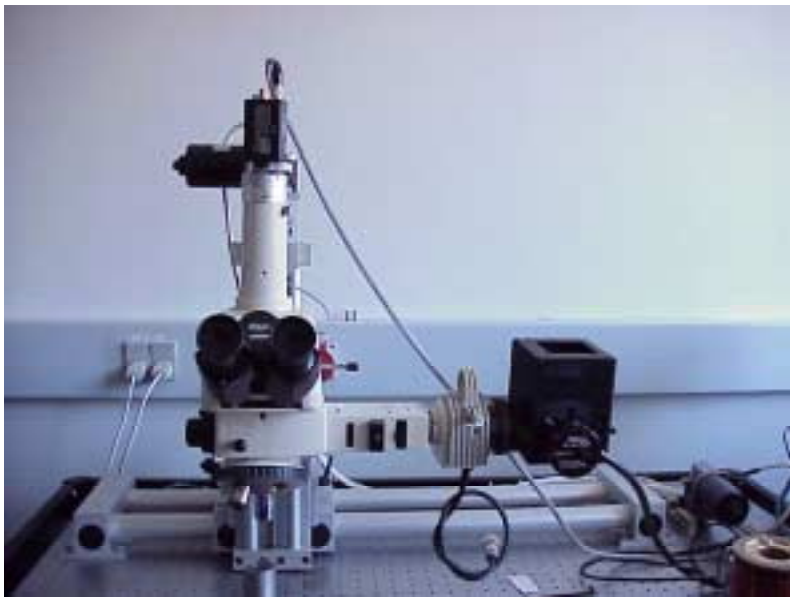

Figure 2.7: The microscope with the CCD camera.

The microscope is an optical stereo microscope from Nikon. The light source is a Hg-lamp with 200 hours lifetime. The light from the lamp is quite intense, and care should be taken no to look in the microscope for long periods. The light from the lamp goes through a heat filter and two green filters with a bandwidth of approx. 50 nm centered at 550 nm. (If no heat filter is used, the intense light from the Hg lamp will burn a hole in the polarizer.) The light then goes through a pinhole with a diffuser before it reaches the first polarizer with an adjustable polarization angle. After another pinhole, the light reaches the semitransparent mirror that sends the light down into the objective. Several objectives can be mounted in the tubular on the microscope. Objectives with magnification of ×2.5, ×5, ×10 and ×20 exist. Due to the space restrictions from the magnetic field coil only 2 objectives can be mounted at the same time. The light from the objective hits the MO indicator and is reflected from the mirror on the back of the MO indicator chip. The reflected light goes through a fixed-angle polarizer and a ×0.45 lens before reaching the C-mount adapter where the CCD camera is mounted. The entire microscope is mounted on a motorized stage.

The CCD camera is a SONY XC-75CE ½". It is black and white, has 768×576 pixels and 8 bits resolution. Both the power to the camera and the data output come through the one cable connecting to the camera. Power to the camera is supplied from a small power transformer. On the camera is a small switch and a potentiometer. The switch determines the type of gain, which is used. It should read M for manual, where the gain then can be adjusted by the potentiometer. If it reads 'A' for automatic the intensity of the CCD picture will be adjusted to give maximum contrast. This is useless when the information we want is in the absolute value of the intensity.

Through the cable to the CCD the data is transferred to the framegrabber in the computer. The framegrabber is a Coreco Tci-SE framegrabber. The configuration program for the framegrabber is called Oculus Tci. (see appendix B4). The framegrabber card and software is installed in the measurement computer, which is a 450MHz PentiumII with 512MB RAM.

The images are recorded using the MTCi program purchased from Unit One. This can show the image live and grab a single frame and save it as .tif, .bmp or .jpg files. The system can also record sequences of pictures with 50 frames per second. This feature has not been used yet.

A custom-made extention to MTCi enables the operating system Tascom [18] to control the MTCi program. Therefore it is possible to record and save pictures taken by the CCD camera from within Tascom. This is very useful since it enables command files in Tascom to be written which sets the field and the temperature and takes a picture and saves it.

2.4 Magnetic field and magneto optical indicator film.

The active layer in the magneto-optical indicator films is ferrimagnetic Bismuth doped yttrium-iron garnet (Bi:YIG). The Bi:YIG layer is grown on a Gadolinium-Gallium-Garnet substrate. On top of this is a thin Al-layer which acts as a mirror for the light that has just passed through the active layer. The mirror is covered by a thin protective Ti-TiN layer.
In the Bi:YIG layer the magnetic spins order spontaneously in the plane of the garnet film. An applied field perpendicular to the film tilts the spins out of the plane. This tilt results in the velocity of right- and left handed circularily polarized light being different. Therefore linearly polarized light propagating parallel to the component of the magnetic field normal to the plane will turn its polarization vector by an angle, θ, which is given by:

$$\theta = VlH$$

where l is the length of the optical path in the film (in the mirror geometry, this is $2t$, where t is the film thickness), H is the local field strength and V is the Verdet constant, which is material specific. Once the spins are tilted 90° an increase of the field cannot give rise to any further rotation of the polarization vector, and the indicator film has saturated. The saturation varies from 50-100 mT for our indicator films. In principle, only the field component perpendicular to the indicator is imaged. There is a small mixing in of the field strength in the plane of the film as shown in [12] but this is normally ignored. The Verdet constant is strongly wavelength dependent with a maximum around 500 nm green light. This is why the microscope has 2 green filters mentioned above.
The Verdet constant is also temperature dependent. But experimentally we have found that the differences below 110K are insignificant.

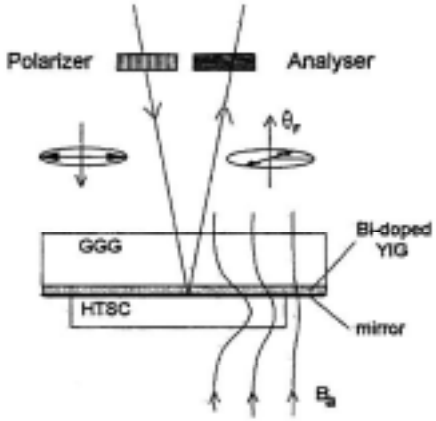

Figure 2.8: Schematic structure of MO indicator film. From [5]

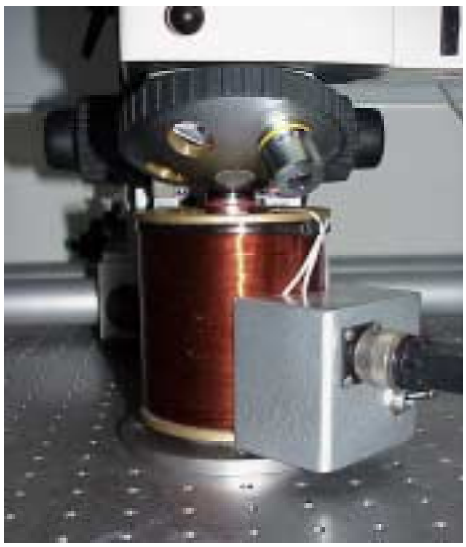

Figure 2.9: Closeup of the coil and microscope during measurements

The magnetic field is applied to the sample and the MO indicator film using a cylindrical coil which fits around the cryostat and allows the microscope to focus on the MO film as seen in figure 2.9.
The coil has 2340 windings and gives 24.6 mT per Ampere. The maximum current that can be sent through the coil is approximately 5 A, giving a maximum field of 123 mT. This should only be done for short periods of time since the coil heats to 80°C within 2 min. at this current (see appendix B3). The current direction in the coil can be changed by a switch attached to the coil.
The current supply is a Delta Electronics SM 70-22 with a maximum current output of 20 A and a maximum voltage of 70 V. It is connected to the measurement computer through a IEEE controller named PSC44M also from Delta Electronics [19]. This controller has GPIB address 4. To change the current supply from remote mode to manual mode, two dip-switches must be set on the back of the current supply. A Tascom driver has been written so commands to the current supply can be sent from within Tascom. It is therefore possible to record and set the current and thereby the applied magnetic field from a command file from Tascom. Details on Tascom can be found in appendix B9 and the Tascom manual [18].

3 RESULTS

3.1 Introduction

In this chapter different examples of measurements with the Magneto optical system is presented. Magneto optical images will be shown of $NdBa_2Cu_3O_x$ crystals, $YBa_2Cu_3O_x$ thin films, single filament $Bi_2Sr_2Ca_2Cu_3O_x$ tapes, and multifilament $Bi_2Sr_2Ca_2Cu_3O_x$ tapes in both flat and cross section configuration. Furthermore, the current density map calculated using Petriina Paturi's inversion program based on the model by Wijngaarden [11] will be shown for $YBa_2Cu_3O_x$ thin film and multi-filament $Bi_2Sr_2Ca_2Cu_3O_x$ tapes.
All the following pictures are taken using the MO setup at the Department.

3.2 Background correction

It is imperative to have a background measurement corresponding to each data image taken. A background measurement consists of a series of images with the applied magnetic field varying between zero and the maximum possible field. The images should be taken with no sample present but with settings identical to the data images. The settings in question are the angle of the polarizer, the gain of the CCD camera, and the mirrors and lenses in the Hg-lamp. With a superconducting sample this is easily obtained by heating the sample above T_c and keeping the rest of the system unchanged. As mentioned in chapter 1, the Verdet constant is temperature dependent, but we have found for our films that no significant change is seen below 120 K
The use of a background measurement is two fold. First to clean the data image of signal due to local defects of the MO indicator and uneven light distribution, and secondly, to provide the conversion from an intensity map to a magnetic field map.
To correct the data image, first the bias of the CCD camera must be substracted. This is the intensity seen in a picture with zero applied magnetic field and it stems from the bias of the CCD chip (or incomplete crossing of the polarizers). This intensity must be substracted from both the data image and the background image. Then the average intensity of the background image with the same applied magnetic field as the data image is found. The background image is normalized with this value. Then the data image is divided with the normalized background image. By

making the correction this way, the absolute intensity of the data image is preserved in good data points, whereas defects are multiplied up to fit the levels in the data image. This procedure assumes that the intensity of the defects is still proportional to the applied magnetic field, but with a different factor than the good areas of the film. An example of this image correction is shown in figure 3.1.

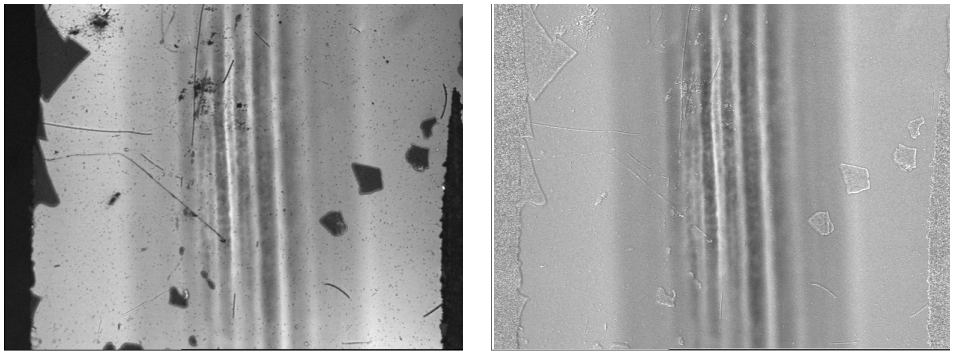

Figure 3.1. Raw data image and corrected image of a 55 filament $Bi_2Sr_2Ca_2Cu_3O_x$ tape at 123 mT and 7 K. See also paragraph 3.6.

The second use of the background images is to determine the dependence of the magnetic field on the observed intensity in the images. With no sample present, the intensity in the background image corresponds to the applied magnetic field. By taking the average value over the MO indicator film of the intensity for each applied magnetic field and plotting it against the applied field a curve like the one seen in figure 3.2 is obtained.

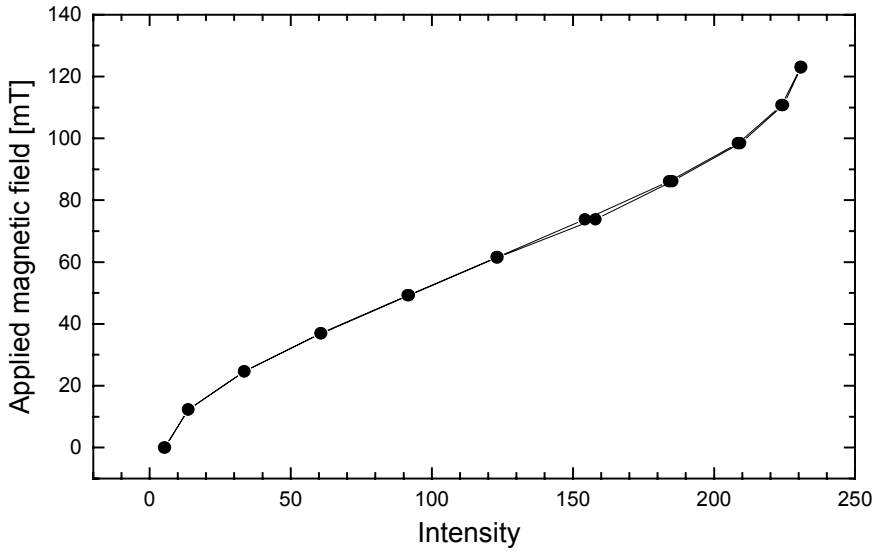

Figure 3.2: Average intensity of background images as a function of applied magnetic field.

To make the conversion from intensity to magnetic field for the data image we need a function that has been fitted to these points. Since the MO image shows the components of the polarization vector of the light, which is perpendicular to the incoming light and the rotation angle is

proportional to the magnetic field a possible assumption for a fitting function is:

$$I = p_1 \sin(\frac{H - p_2}{p_3}) + p_4 \quad \Rightarrow \quad H = p_3 \arcsin(\frac{I - p_4}{p_1}) + p_2$$

where I is the intensity, H is the applied magnetic field and p_1-p_4 are fitting parameters. Although physically correct, there is a mathematical twist to using this fitting function, due to the fact that the argument of the arcsin function must be less than or equal to one. Some care must be taken to ensure that this is true for the entire data image. An alternative fitting function suggested by T. Frello [5] is:

$$I = A_0 + \frac{A}{1 + \exp(\frac{B - B_0}{dB})} \quad \Rightarrow \quad B = dB \ln(\frac{A}{I - A_0} - 1) + B_0$$

where I is the intensity, B is the applied magnetic field and the rest of the variables are fitting parameters.
With the fitting function the data image can be converted to a map of the local magnetic field. This can then be converted to a current density map using e.g. the Wijngaarden method. Examples of data images and current density maps will be shown in the following.

3.3 $NdBa_2Cu_3O_x$ crystal

The first measurements with the magneto optical setup where performed on a $NdBa_2Cu_3O_x$ single crystal. A superconducting high-T_c sample cooled below T_c will expel all magnetic field from its interior when it has been cooled in zero magnetic field and an external magnetic field is applied.
In figure 3.3 is the image taken of the crystal after cooling in zero field to 7 K and applying a magnetic field of 123 mT. No background correction is performed. The edge of the indicator film is seen as the straight line to the right of which all is black. The outline of the crystal is clearly seen, and the black interior indicates that the crystal has expelled magnetic field from its interior. The graph shows the intensity along a line diagonally across the crystal. The intensity in the center of the crystal is close to zero, and is mostly offset from the CCD camera. Just outside the crystal the magnetic field is larger than the applied magnetic field due to the expelled field from the superconductor. Unfortunately, the MO indicator is not large enough to show the intensity flattening to the applied field value and no background image was taken to show what the unperturbed intensity at this field is.

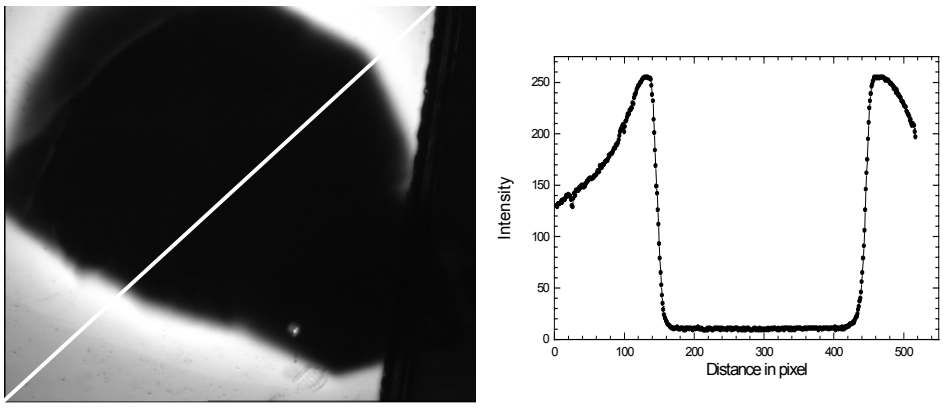

Figure 3.3: MO image of a $NdBa_2Cu_3O_x$ crystal zero field cooled to 7 K with an applied field of 123 mT and a profile diagonally over the picture

The same crystal is then cooled in a field of 73.8 mT from above T_c to 10 K. Then the external field is ramped down to zero and the image seen in figure 3.4 is obtained. Clearly, the crystal is trapping the magnetic flux in its center. The field strength falls of close to the edge of the crystal. The intensity seen just outside the crystal must be of opposite sign to the field inside the crystal since it is the returning field lines. Far away from the crystal, the intensity falls of almost to the CCD background.

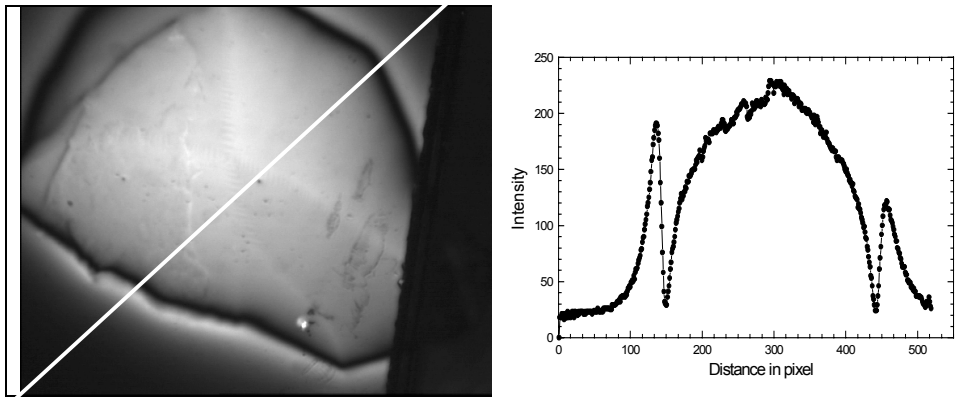

Figure 3.4: MO image of a $NdBa_2Cu_3O_x$ crystal field cooled at 73.8 mT from above T_c to 10 K a profile diagonally over the picture

Depending on the pinning strength of the crystal, the trapped flux will decay in time. At this low temperature no significant time dependence of the field configuration is observed. Keeping the external field zero the crystal is now heated. Around 40-50 K the flux starts to redistribute. The flux configuration around 40 K is seen in figure 3.5.

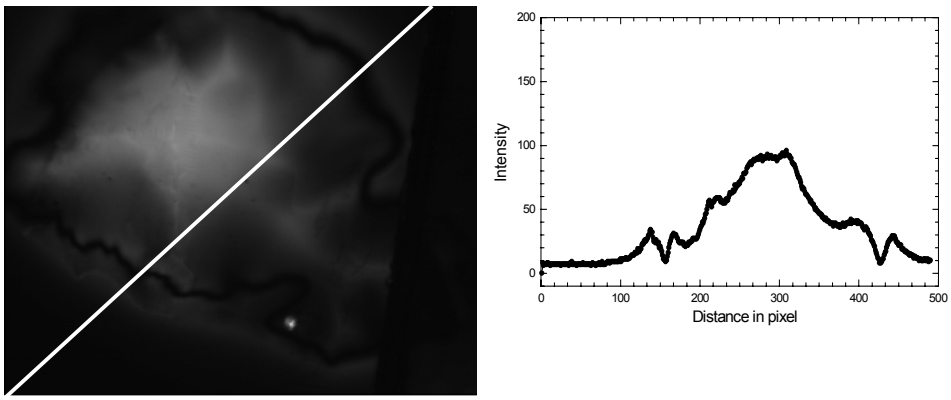

Figure 3.5: MO image of the $NdBa_2Cu_3O_x$ crystal, field cooled at 73.8 mT from above T_c to 10 K and then heated to 40 K. The profile shows the intensity diagonally over the picture. The black line is the boundary between the different signs of flux. It is seen that a weak or thin part of the crystal exists towards the right of the image. Flux penetrates easier here than in the rest of the crystal.

3.4 $YBa_2Cu_3O_x$ thin film patterned in parallel stripes

One aim of the magneto optical setup is to be able to extract the local current density of e.g. superconducting $Bi_2Sr_2Ca_2Cu_3O_x$ tapes or $YBa_2Cu_3O_x$ coated conductors. In this paragraph we look at a model system which is geometrically simpler than the tapes. The model system consists of well-defined stripes of $YBa_2Cu_3O_x$ thin film. The thickness, width and length are then known quantities. This can be used as a test system both for the imaging and MO indicators as well as a model system to perform magnetic field to current density inversion on.

Laser ablated $YBa_2Cu_3O_x$ thin films with T_c close to 92 K and thickness of 200 nm were fabricated on a substrate of MgO at NKT Research A/S. Using e-beam lithography several geometries with varying stripe width and stripe distance were made in order to investigate the coupling between neighboring stripes. Here are shown images for stripes that are 220 μm wide and spaced 200 μm apart.

To correct for uneven distribution of the light in the microscope, local defects in the MO films and offset in the signal from the CCD camera, a background image at the same magnetic field but with a temperature above T_c (here 100 K) is used.

Figure 3.6 shows the corrected images for T=44 K and applied fields between zero and 123 mT. The shielding of the field by the superconductor is clearly seen in the images for low fields. As the field increases, the characteristic roof top field distribution of field is evident. This arises due to the fact that the current flows parallel to the edges and changes direction sharply at the corners.

H = 12.3mT

H = 24.6mT

H = 36.9mT

H = 49.2mT

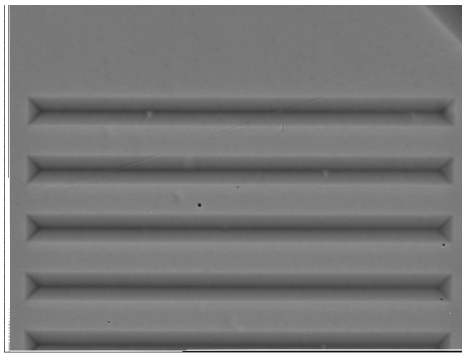

H = 61.5mT

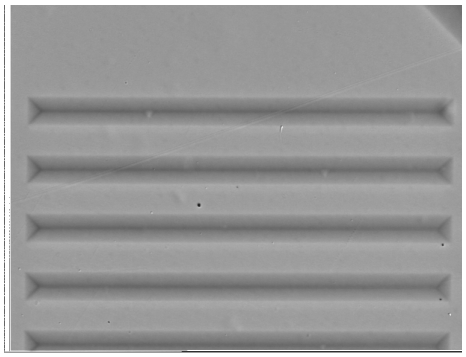

H = 73.9mT

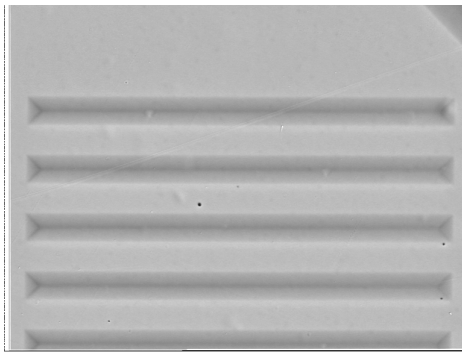

H = 86.1mT

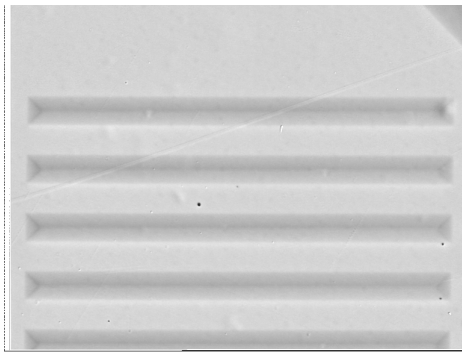

H = 98.4mT

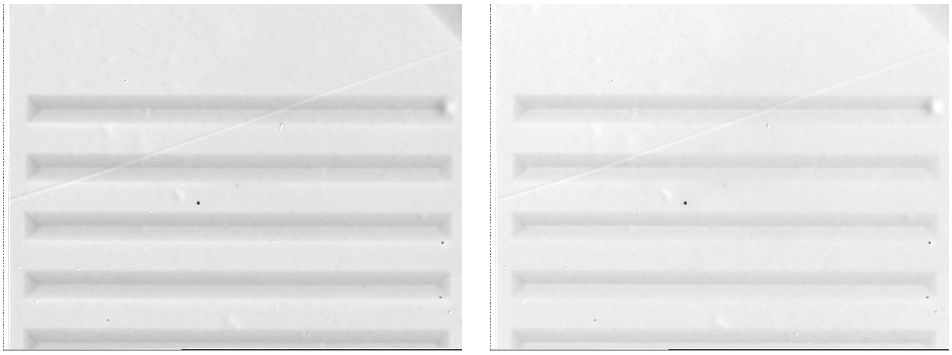

H = 111mT H = 123mT

Figure 3.6 MO images of $YBa_2Cu_3O_x$ thin film at T = 44 K and varying applied field.

In figure 3.7 the average magnetic field strength along a line perpendicular to the strips is shown for different applied magnetic field. The partial penetration of the magnetic field is seen for the small applied magnetic field. The focusing of the field just outside the superconductor is clearly seen. A slight discrepancy from the triangular shape predicted by the Bean model is observed. The shape of the field strength is in good agreement with the model for thin samples suggested by Zeldov *et al* [6]

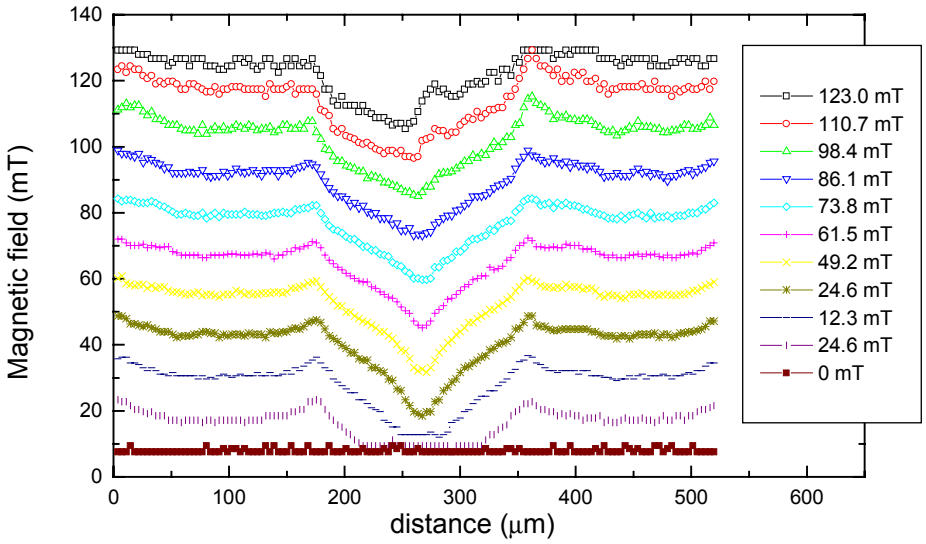

Figure 3.7: Field profiles along a line perpendicular to the strips for varying applied magnetic field at 44 K.

At about 50 mT there is full field penetration at 44 K. Figure 3.8 shows the average magnetic field profiles for a fixed applied magnetic field and varying temperature. For each measurement the superconducting sample is heated above T_c, zero field cooled, and then the field is ramped to 49.2 mT and the image is recorded. The variation in trapped flux with temperature is clearly seen. The focussing of the field just outside the superconductor is clearly seen.

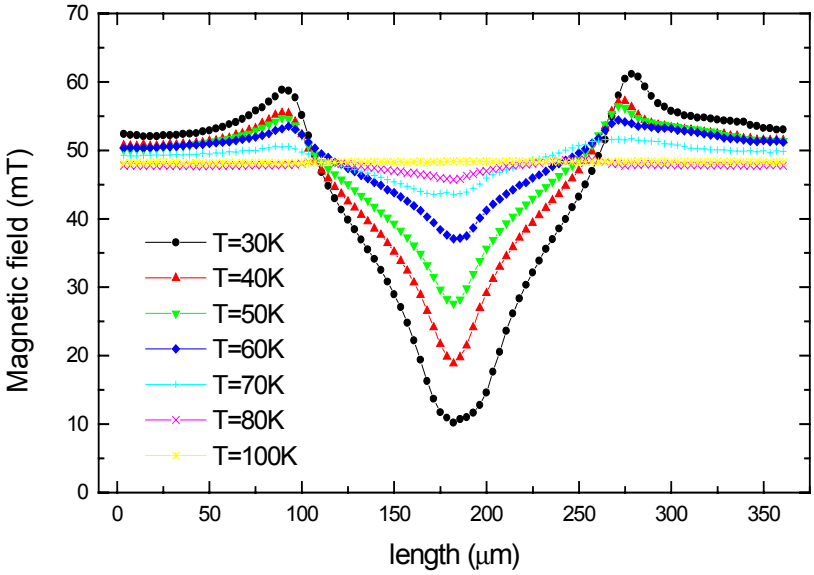

Figure 3.8: The field profiles for an applied field of 49.2 mT and different temperatures.

Using the Wijngaarden method, the MO image for 44 K and 49.2 mT is converted to a map of the current density. The film thickness is 0.06 pixels (found as 200nm divided by 3.66μm/pixel for the ×5 magnification used). The distance between the MO indicator film and the sample is assumed to be 1 pixel = 3.66 μm. Fig. 3.9 shows the average current density in the directions of the stripes along a line perpendicular to the stripes. The average j_c is found to be around $7 \cdot 10^{11}$ A/m^2.

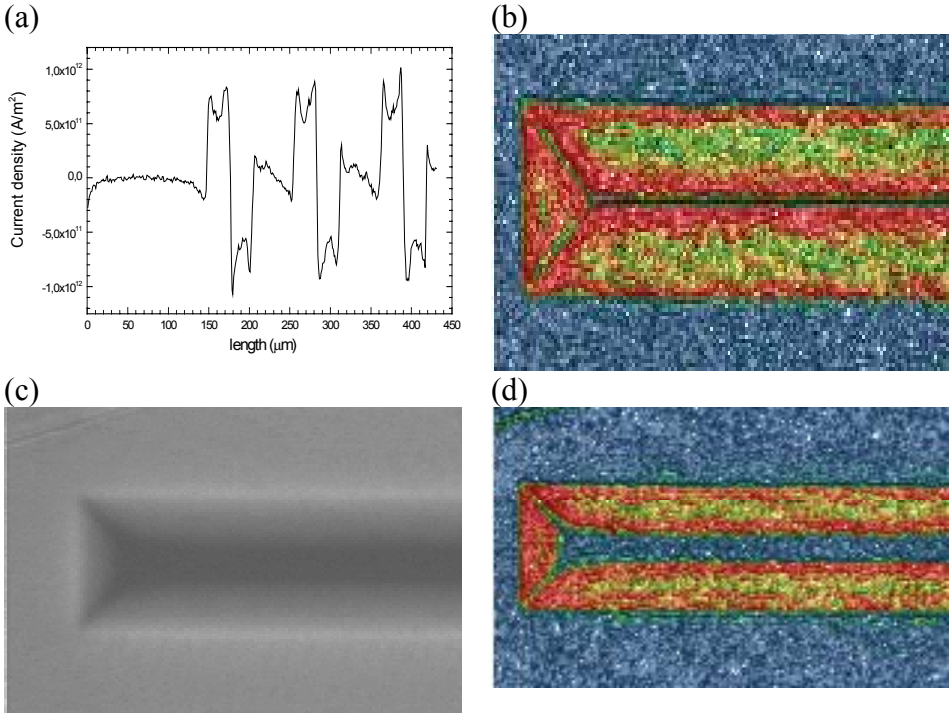

Figure 3.9: (a) Current density along a line perpendicular to the stripes for 44 K and 49.2 mT. (b) Current density map of one end of a superconducting strip. (c) Intensity map for 44 K and 24.6 mT. (d) Current density map for 44 K and 24.6 mT

3.5 $Bi_2Sr_2Ca_2Cu_3O_x$ single filament tapes

A small piece of single filament $Bi_2Sr_2Ca_2Cu_3O_x$ tape is polished until the silver is removed from one side. The MO indicator film is placed directly on top of the exposed $Bi_2Sr_2Ca_2Cu_3O_x$. This ensures that the indicator film is as close to the sample as possible, thus giving a better spacial resolution. Figure 3.10 shows the MO image obtained at an applied field of 135.3 mT on the zero field cooled tape. The temperature is 8 K. No background correction has been made. The piece of tape is approximately the same length as the MO indicator. The shielding effect of the tape is clearly seen. A roof-top pattern can be seen. The flux penetration is seen in areas with weak current carrying capability. They are arc shaped and agree with rolling cracks known to occur in single filament tapes.

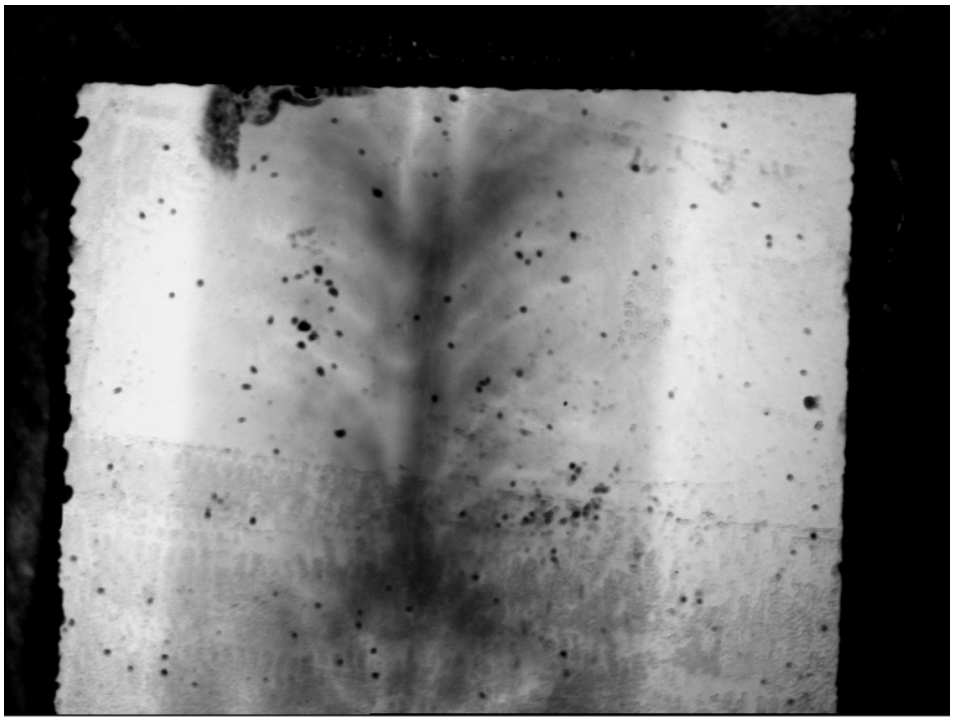

Figure 3.10: MO image of single filament tape zero field cooled to 8 K. Applied field is 135.3 mT

3.6 $Bi_2Sr_2Ca_2Cu_3O_x$ multi filament tapes

In a collaboration between the Department of Manufacturing Engineering from DTU, Nordic Superconducting Technology A/S and Risø, tapes with different number of filaments and two different flat rolling techniques were investigated. The 6 different tapes had 37, 55 or 85 filament and were either rolled from round (the standard procedure) or rolled from a square tube, which was made in the last drawing step.
One aim of this was to make tapes with different thickness of the individual filaments. The heat treatment of each type of tape was individually optimized. The average thickness of the individual filaments was 13 μm, 11 μm and 8μm for 37, 55 and 85 filament respectively. The thinner the filaments the shorter were the sintering times needed to optimize the

tapes. Furthermore, the spread in the thickness of the filaments and the overall filament homogeneity were better for the square rolled tapes than for the standard round rolled tapes. This effect is more pronounced the fewer the filaments.
Figure 3.11(a) and (b) show the MO images for round rolled and square rolled tapes with 37 filaments. In figure 3.11(c) and (d) are photographs of the cross section of the tapes. The cross section picture is taken at a different point of the tape than the MO images, but is gives an indication of how the filaments are distributed in the section of the tape in question. Figure 3.11(e) and (f) shows the average intensity distribution along a line perpendicular to the filaments. From the background images it is found that the MO indicator is far from being saturated and the intensity of these pictures are in the linear part of a curve similar to 3.2. This means the intensity variations approximately describe the magnetic field variation.

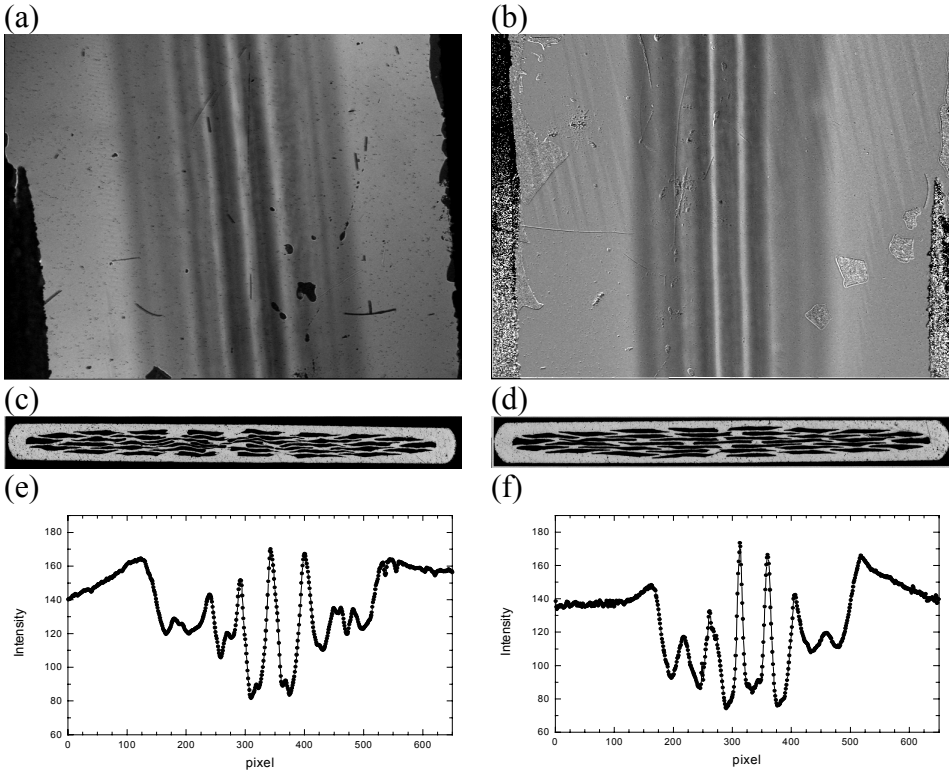

Figure 3.11: (a) MO image of 37 filament tape rolled from round (b) MO image of 37 filament tape rolled from square. In both images T = 6 K and the applied field is 123 mT. (c) Average intensity profile for the round rolled 37 filament tape. (d) Average intensity profile for the square rolled 37 filament tape

In the MO images the shielding from the individual filaments are clearly seen. The individual filaments seem to have a homogeneous shielding along the filament. From the cross sections it is seen that for both the round rolled and square rolled 37 filament tape there are 7 to 8 filaments in the top layer of the cross section. The MO image will record mostly the signal from the closest filaments since the magnetic field from a current line falls of as 1/z (see chapter 1). In the intensity curves 7 to 8 min-

ima are seen. The filaments, which are not in the top layer, are not seen in the image. In the round rolled tape the central minimum are deeper than the edge minima whereas the minima for the square rolled tape are closed to equal depth.
The effect could be due to either a larger current density in the center filaments or that the center filaments are closer to the MO indicator than the edge filaments. The tapes have been polished before the MO images were taken. But looking at the cross section pictures, it is clear that the variation in the depth of the filaments is not enough to account for the variation in the field strength observed. Therefore the edge filaments in the round rolled tape must have a lower j_c than the center filaments, whereas the square rolled filaments have more of less the same j_c. No absolute comparison of the j_c of the round rolled and square rolled tapes will be attempted here since the intensity of the MO images (and thus the value of the calculated j_c) will depend on the filament to MO indicator distance. A more thorough measurement and analysis would be needed to make such a comparison.

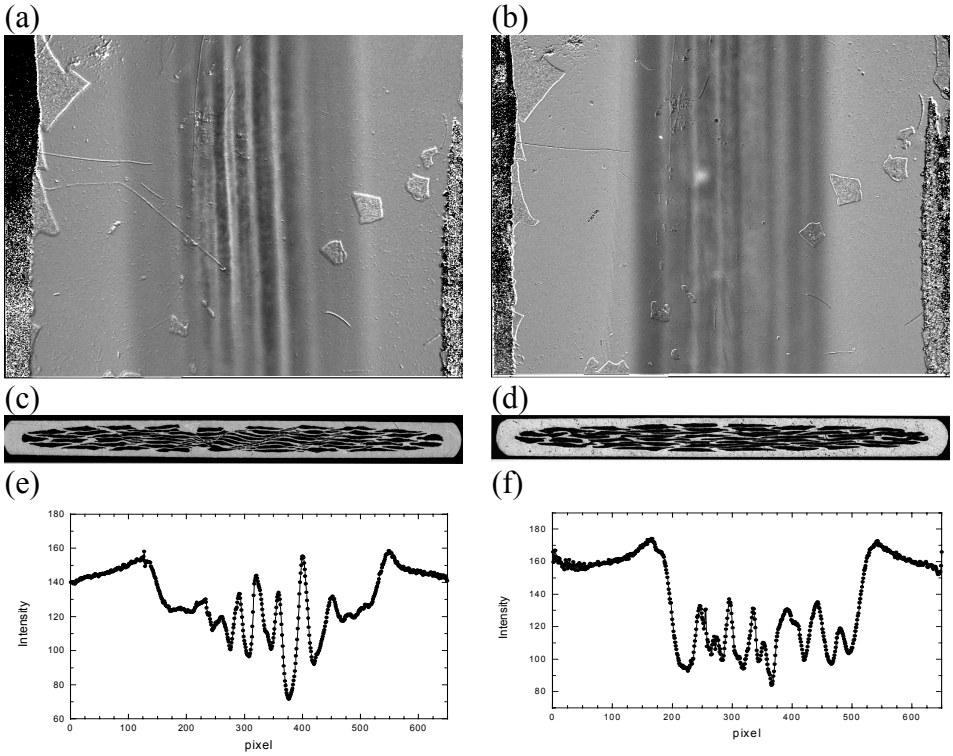

Figure 3.12: MO images of 55 filament tape rolled from round (a) and rolled from square (b). In both images T = 7 K and the applied field is 123 mT. (c) Average intensity profile for the round rolled 55 filament tape. (d) Average intensity profile for the square rolled 55 filament tape

Figure 3.12 and 3.13 show the same images for the 55 filament tapes and the 85 filament tapes. Similar conclusions about the difference between the round rolled and square rolled tapes are obtained from these.
Both the 55 and 85 filaments round rolled tapes show a granularity of the filaments in the MO image. This could indicate that there is bad inter-

grain connectivity in the filaments. This is not seen in the 37 filament round rolled tape.

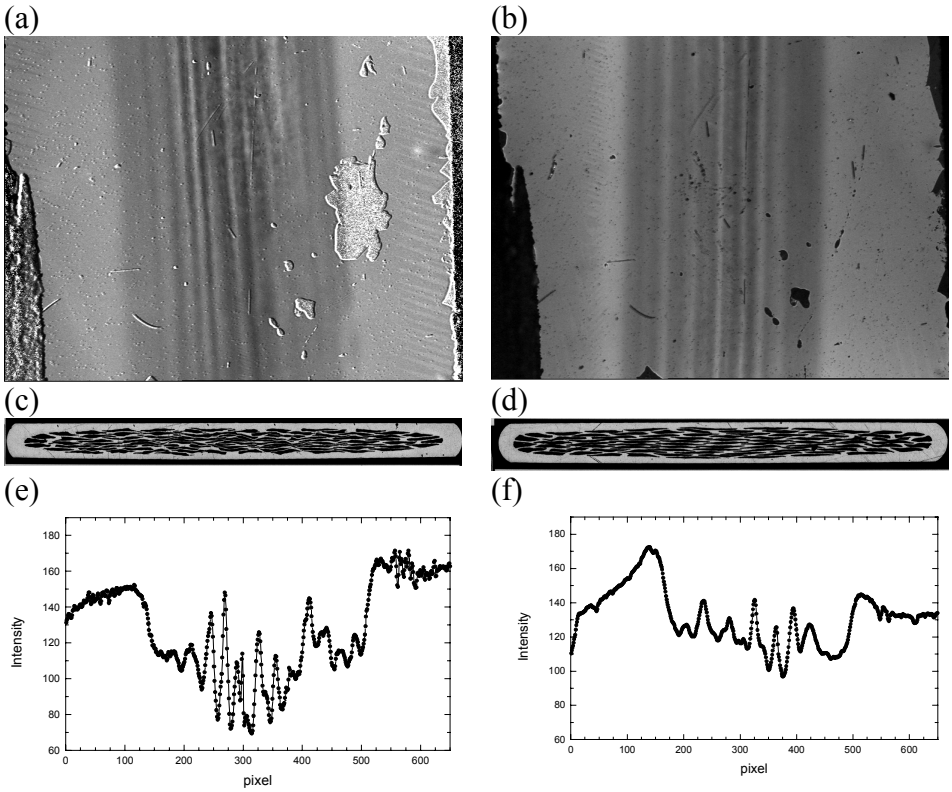

Figure 3.13: (a) MO image of 85 filament tape rolled from round (b) MO image of 85 filament tape rolled from square. In both images T = 6 K and the applied field is 123 mT. (c) Average intensity profile for the round rolled 85 filament tape. (d) Average intensity profile for the square rolled 85 filament tape

In figure 3.14 is a current density map of the round rolled 55 filament tape calculated from the image in 3.12(a). The thickness of the sample is assumed to be 1 pixel = 7.2 μm and the distance to the MO indicator is assumed to be 1 pixel = 7.2 μm. It is seen that the current density is granular along the filaments. The scratches and defects of the MO film are still visible, so a better image correction should be attempted.

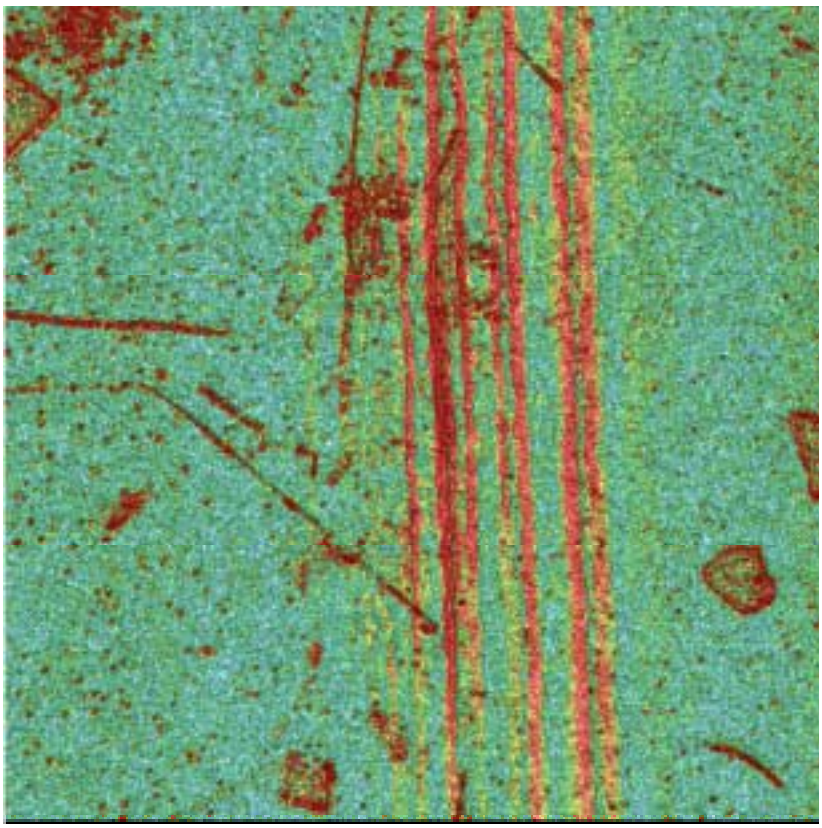

Figure 3.14: Current density map of a 55 filament tape

3.7 $Bi_2Sr_2Ca_2Cu_3O_x$ multi filament tapes - cross section

Multi filament $Bi_2Sr_2Ca_2Cu_3O_x$ tapes was studied in cross section with the MO technique by Michael Koblischka during his stay at Risø. The cross section study enables the study of filament quality as a function of their position in the tape.

Fig. 3.15 shows the magnetic field patterns of a cross-section of a tape with 37 filaments. The field is oriented parallel to the filaments. Several dark areas along the Ag sheath is seen. These dark areas are the shielding filaments. The number of shielding filaments are less than the 37 filaments that are present. It seems that the filament in the center is shielding less than the filaments along the edge of the tape [20].

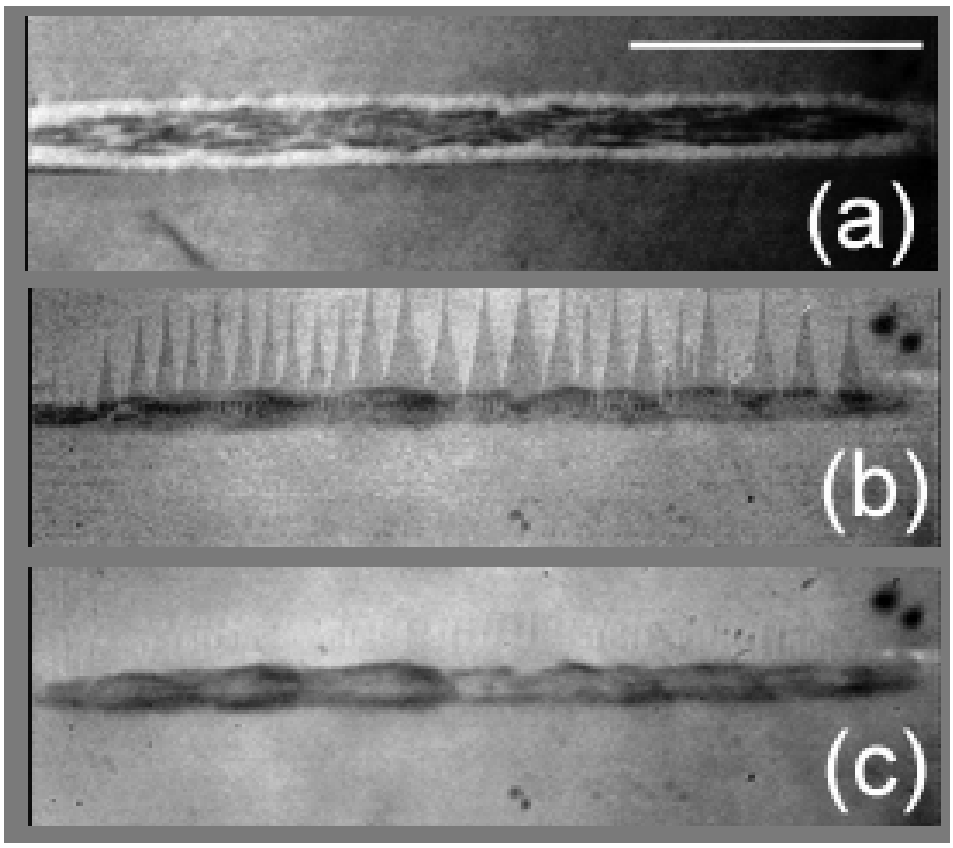

Figure 3.15. Flux patterns of a cross-section of a 37 filament Bi-2223 tape, T = 7 K and the field applied parallel to the filaments. (a**)** optical polarization image of the cross section of the tape, (b) MO image at 20 mT, and (c) MO image at 50 mT. Marker = 1 mm

A. USER GUIDES

A.1 Step-by-step user guide for measurement with the system

RISØ	Magneto-Optic Setup User guide	Britt Hvolbæk Larsen March 2000

1. Mounting sample

- Mount the sample on a sample holder using e.g. conducting carbon cement or cryocon. This can be dissolved in acetone.
- Do polishing if needed.
- Screw the sample holder into the cryostate using the tool. Use a little thermal grease on the bottom of the holder to ensure good thermal contact.
- Place the MO film on top of the sample. No glue or grease is used.
- Mount outer vacuum shield and ensure that the window is situated correct.
- Open the valve to the vacuum pump and start the pump - remember to close the release valve on the turbo pump.

2. Cooling

- The cooling procedure can begin immediately, since the temperature of the cryostat will not drop in the first ½ hour. The base pressure of about 10^{-5}mbar is reached before.
- Insert the bayonet into the transport dewar. Close the valve on the dewar leading to the evaporation line and disconnect the tube from the He collection system.
- Connect the flowmeters to the He collection system and open the 2 flowmeters fully.
- Connect the pressure tank to the bayonet. Pressurize the transport dewar to 5 psi = 0.351 kg/cm^2. This corresponds to the pressure of the safety valve on the bayonet.
- Turn on the cryostat shield heater - this gives about 50°C at the lower part of the cryostate.
- During the first part of the cooling the flowmeters will read approx 15mm. When the system gets cold the rate will be approx 50mm.
- The nob for the needle valve at the bottom of the cryostate should be approximately 4 turns from fully closed to reach the base temperature.
- The total cooling time is about 1 hour. The first ½ hour the transfer tube cools, and no cooling of the cryostate is seen. When the cryostat is cold the flow is about 50mm in both flowmeters.
- To pump on the He in the cryostat, close the valve before the tip flowmeter, open the valve to the right on the He pump panel, open the valve from the He pump to the He collection system and turn on the pump. The pressure gauge reads about 200-300 mbar. A larger pressure difference can be obtained by closing the nob at the bottom of the cryostate.

3. Start-up of system

- Turn the computer on.
- Start Tascom. (use the icon or c:\tascom\tassup2\tascomsu.exe)
- Start the framegrabber software mTCI (use the icon or C:\winnt\twain_32\mtci\mTCI.exe). Press 'grab' to have the picture update continously.
- If the temperature controller has been restarted, the thermometers must be initialized by running the command file 'moinit' from TASCOM. The temperature can be checked by ?temp5 for the control temperature and ?temp6 for the sample temperature.
- Make a subdirectory in d:\data where your datafiles will be saved. In TASCOM write >data_dir='name' to get TASCOM to save the files in this directory. Ignore the error message.
- Set the filename using >fina='name'. A maximum of 6 characters can be used (?). Set the file number by >segn=0. Datafiles with then be saved as name000n.dat, where n is increased automatically for each datafile. To add text in the top of the datafile use the command dfit="text in file".
- Set seccd=0. This is the number for the .tif files saved from TASCOM as name000m.tif in the data_dir directory.

4. Measurements

- Use the command file 'templine' to measure a temperature profile (e.g. during cooldown). It output T5 and T6 to a file with an interval of N seconds between temperature readings.
- Turn on the Hg lamp power and press ignition until a green light is seen from the filters after the lamp.
- Place the coil over the cryostate.
- Choose with objective to use and move microscope in place. The XYZ motors works if the microscope is maximally away from the table. Move the last distance in z manually.
- Adjust optics so polarizers are crossed and the image is in focus on the computer screen (differs from microscope focus)

Temperature control

- To set the temperature use the following TASCOM commands : > tc'set6=100' (setpoint of thermometer 6 closest to heater is set to 100K) and >tc'vcc6=on' (turns on temperature controller to thermometer 6).
- To stop the temperature regulation use: >tc'vcc6=off'

Magnetic field

- The magnetic field can be swept up and down using the command file 'magloop'. It prompts for the parameters BBEG, BEND and DB, which is the start current , maximum current and step size in ampere. The conversion factor of the coil is 1A = 246Gauss = 24.6mT. The command file magloop takes a picture for each field value
- To adjust magnetic field manually, initialise the current supply with the command psc44'fu70,fi20'. Then set the current to e.g. 4A using psc44'i',4.
- The current to the coil should not exceed 5A, and should only be held at 5A for short times. The coil with heat to 80°C in 10min at 4A and in less than 5min at 5A.

Pictures from TASOM

- Use >snap to take a picture from TASCOM.
- Use ccd_save to save the picture manually.

5. Cold swap

Changing samples while cryostate is cold

- Close the valve to the vacuum pump.
- Connect the He pressure tank (or if present N2 tank) to the inlet with the green valve just above the vacuum pump valve. Before connecting, adjust to a steady flow.
- Cover the cryostate with the glove box.
- Open the green valve to let He gas into the vacuum space of the cryostate. There should be a hearable flow of gas out of the cryostat.
- Remove window and sample and place new sample.
- Place window
- Close He flow
- Start vacuum pump.
- Keep glovebox in place until low pressure is reached. If the outside of the cryostate ices anyway, use a heatgun and wipe off moisture.

6. Ending measurements

- Close the flowmeters.
- Turn off cryostate shield heater.
- Close valve to vacuum pump and turn off vacuum pump. Ventilate the turbo pump using the small screw on the side of the turbo pump.
- If measurement is to continue later that day, leave cryostate pressurized and bayonet inserted.
- If measurement is to continue the next day, leave bayonet in transport dewar, but connect the dewar to the He collection system and let out the pressure.
- If the system will not be used for several days, depressurized the dewar and take the bayonet up.
- Keeping the cryostate under vacuum and having turned everything off, the system can be left to itself to heat up.

A.2 Step-by-step user guide for data analysis

RISØ	Magneto-Optical Setup image processing	Britt Hvolbæk Larsen Petriina Paturi Dec 2000

7. Measurement

- For each picture there should be a background picture for the same field. This should be measured above T_c without moving the microscope or touching the polarizer.

8. ImagePro

- Convert the RBG-tifs to grayscale in ImagePro using 'Edit' and 'convert to'.
- The background picture is aligned to the data picture using the function 'registration' found in the 'process' menu. In the options, use 'translation and rotation' only. Do not use any scaling - this will give different size of pictures. Place at least 4 points on e.g. point-like faults in the film.
- There are now 2 ways of correcting for the background:

3a. Background correction in ImagePro

- Substract the bias. The bias is the pixel value when taking a black picture. It arises from an offset in the CCD. If parts of the picture has no MO film, the pixel-value here is the bias. The bias has been measured to approximately 5. The bias value is substracted from both the data picture and the background picture 'operations' in the 'Process' menu.
- Now we want to divide the data picture with a normalized version of the background picture. The result should be a .tif file, so we need to stay in integers. Convert both the data file and the background file to 16bit grayscale by 'Edit', 'convert to' and choose 16bit and 'copy values without scaling'
- find the average intensity of the background picture, using an AOI and the histogram button, and multiply the data file by this number. Then divide this multiplied datafile with the background file. This corrected file is then converted back to an 8bit file and this is the corrected image.

3b. Background correction using Petriinas Wijngaarden program

- Petriinas Wijngaarden program can also be used to do the background correction. The data picture and the background picture needs to be of equal size.
- use a non-integer bias. (to avoid dividing by 0).

4. Petriina's Wijngaarden program

- The program is a Scilab program. Scilab is available on fys-lin-2.
- Files needed to run the program: wijn_n.sci, wijnfunc_n.sci, gsolve_u (compiled), tiff2sci (compiled).
- (To compile gsolve write gcc -o gsolve_u gsolve_u.c -lm . This need nrutils.c and .h and the toeplz.c)
- Start Scilab by typing >Scilab.
- Start the Wijngaarden program by typing > exec('wijn_n.sci'). Click on the title to begin
- Choose the datafile and click OK. (ex b232g120div232.tif)
- In the Scilab Toggles Panel that appears choose the 'Use tif-file' button if the

background correction has been done in ImagePro as described above in 3a. If part of the analysis has been performed before, choose 'Use previous' for the actions that has been performed. The program saves the intermediate matrices to the disk and can reuse them.

- Give a name which will be the beginning of all the data files. (ex b232g120div232.tif). To write in the scilab windows one needs to click on the white field and keep the cursor in the white field.
- Choose calculation area by clicking opposite corners of the wanted area in the plot window. NB! The area chosen should be approximately square in pixels.
- Give the equation for the magnetic field in mT as a function of the intensity seen on the picture. Use the variable x for the intensity (ex : 42.3*asin((x-116.9)/114)+59))
- Give the sample thickness in units of pixel size. (ex the film thickness is 200nm and the pictures are taken at x5 magnification which has 1pixel = 3.66μm, this gives a sample thickness of 0.06 pixel). Then give the distance from the top of the sample to the MO layes, also in units of pixels.
- When running the program the first time the above will result in an error at this point. Restart the program by typing exec('wijn_n.sci') in Scilab and use 'previous' for 'Remove background', 'choose calc area' and 'calc B'.
- Choose a filtering radius. This is a cutoff radius in Fourier space. For no filtering choose cancel. A radius of 50 has no influence. A filtering radius os 15-20 is good for slightly noisy pictures, and 5-10 is for very noisy pictures. The filtered picture is displayed and the filtering can be redone.
- Now the Jx, Jy and J matrices are displayed and there is a prompt whether you want to save them.
- Now the program is finished.

- Often there are large pixels near the edges, which are not physical. A useful Scilab command is how to make a submatrix from a larger matrix. (ex >temp=J(20:210,10:220))
- To get the current density in units of A/m^2 the J matrices must be multiplied with 1e-3/(4π*1e-7*pixellength), where pixellength is the size of the pixels in meters. (ex >realJ = J*1e-3/(4*%pi*1e-7*3.57e-6))
- Export the wanted data matrix from Scilab using the command >write('filename',matrixvariable). This writes an ascii file with all the numbers (but not ordered in rows and columns) within the directory where Scilab was started.
- At at unix prompt run the matrform perl script by typing >matrform.pl filename xsize ysize. This give an ascii file with 'xsize' number of columns and 'ysize' number of rows named filename.form placed in the same directory as filename. This can then be analyzed by e.g. Origin

useful commands in scilab:
xbasc() - clears the plot window
temp=J(20:210,10:220)
grayplot(1:N,1:M,matrix) - plots a NxM matrix
contour(1:N,1:M,matrix,no-of-contours) or contour(1:N,1:M,matrix,[1,2,3,4,5])
size(J) - gives size of the matrix J
J=read('filename',N,M)

6. Batch version

- There is a batch version of the program, started by >exec('wijnbatch.sci.')
- As input is uses a file looking like:

```
filename="/home/fys/brhl/wijngaarden/data/ybcofilm0012/b232g120div212.tif"
savename="/home/fys/brhl/wijngaarden/data/ybcofilm0012/b232g120div212"
```

```
startX=    100
startY=    10
N=         200
HvsI=      "42.3*asin((x-116.9)/114)+59"
thickness= 0.06
distance=  1
// next line is either "before", "after" or "none"
filter= "none"
filter_r=  7
```

B. SETUP

B.1 Cryostat and pumps

The cryostat is an APD cryogenics model LT-3B-110 open cycle system [16]. It operates with either liquid Helium or liquid Nitrogen. It is equipped with a flexible Z-shaped 10-foot long transfer line. The cold finger is enclosed in a heat shield, which has been modified with a hole to give optical access to the cold finger.

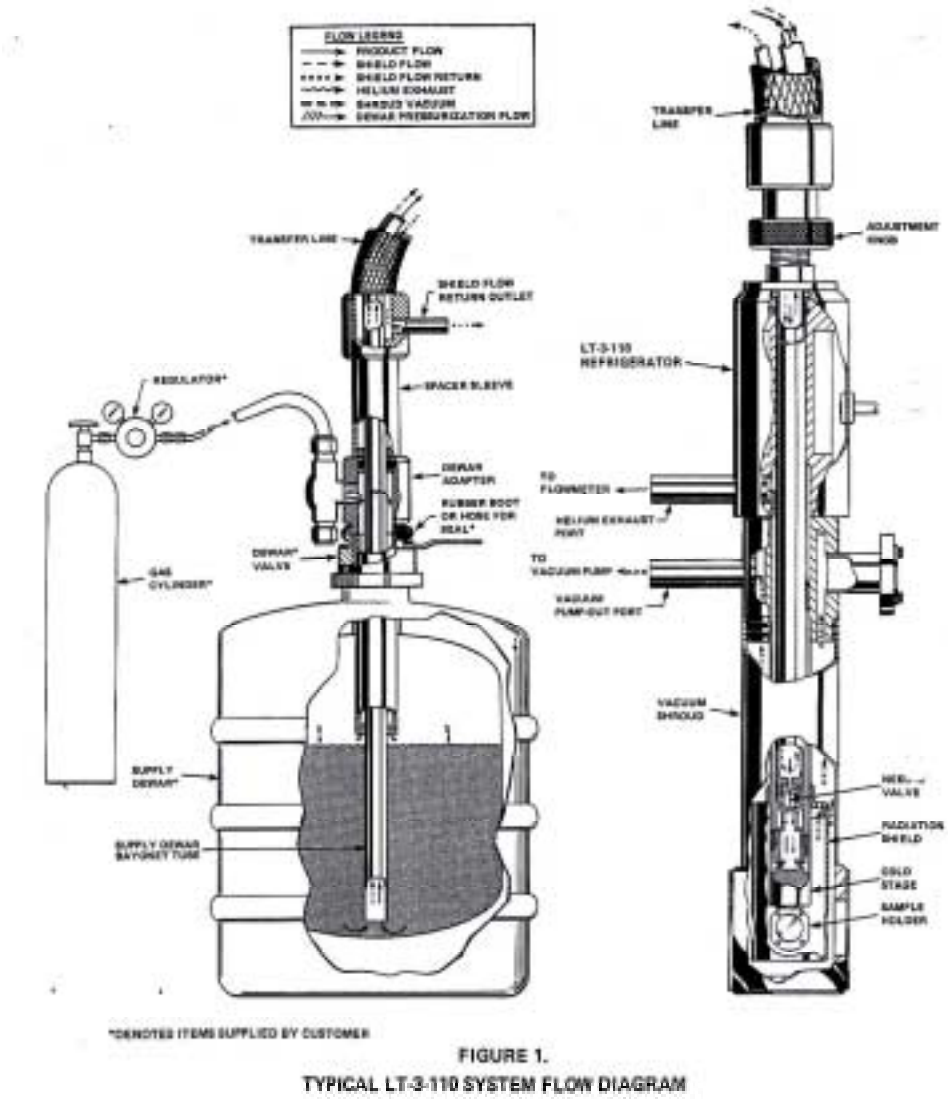

Figure B1.1: Flow diagram of cryostat. From [16]

The cryostat is mounted through a hole in a vibration damped table and fitted with a vacuum shield, which is also fixed to the table. The cryostat is mounted so the cold finger is pointing upwards and the transfer line

connects from below the table. The vacuum shield has a glass window on top with an O-ring to the vacuum shield. The glass window is purchased at Edmund Scientific Ltd. The material is specified in the catalog as B270. The glass disc is 35 mm in diameter and 2 mm in thickness
The transfer line vacuum shield should be pumped to 10^{-4} torr and this should be checked every 12 month
The cool down time of the cryostat from room temperature is approximately 50 min. The temperature of the sample during the cool down is illustrated in figure B1.2. The first half hour the transfer tube cools down, and the temperature of the sample does not change.

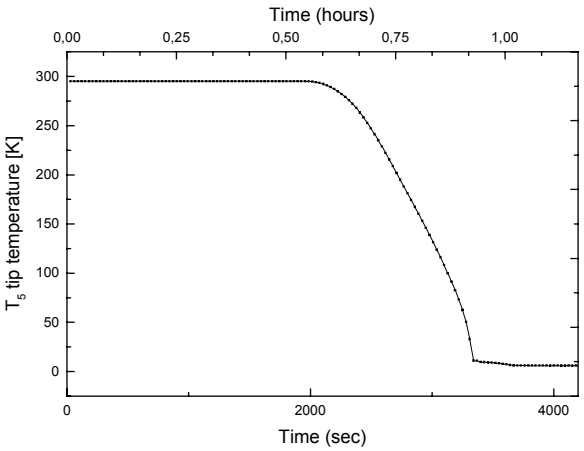

Figure B1.2: Temperature versus time during cool down of the cryostat

The isolation vacuum is provided by a Varian Turbo-DRY 70 pump. The vacuum pump stand is seen in figure B1.3(a). The Helium pump is a Rotary vane pump SD201 with the input side equipped with an oil mist eliminator. It is used to lower the boiling temperature of the liquid Helium to reach the base temperature of the cryostat. The pump stand is seen in figure B1.3(b).

(a) (b)

Figure B1.3: Pump stands as described in text.

B.2 Sample mount and gold plating technique

To ensure that the sample mount has a high thermal conductivity, it is made from OFC (oxygen free copper). Furthermore, after it has been machined, it is annealed for 2.5 hours at 600°C and for 5 hours at 550°C in vacuum or an inert atmosphere like Helium [21]

The gold plating of the heat shield and the sample mount is performed using the following recipe. The surface of the object is cleaned mechanically from oxides. Then it is immersed in an aqueous sulphonate based detergent at room temperature with ultrasound for 1 hour. The object is then washed in distilled water and transferred to a boiling gold plating bath for 10 min. The gold plating bath is prepared by mixing two solutions followed by heating the solution to the boiling point. Solution **A** is a 750ml water solution 0.1M NaOH, and 0.055M NaH_2PO_4. Solution **B** is a 250 ml water solution 0.013M $AuCl_3$ and 0.6M KCN.

The copper discs for the sample mount are made of OPC copper. They are 20 mm in diameter and have a threading of 1 mm per turn (M20×1).
The samples are glued to the copper discs using conducting carbon cement (CCC). Its trade name is Leit-C and it is purchased from:

PROVAC
Fröhrenweg 8
FL-9496 Balzers
Liechtenstein
tel : (075) 388 1945
fax: (075) 388 1949

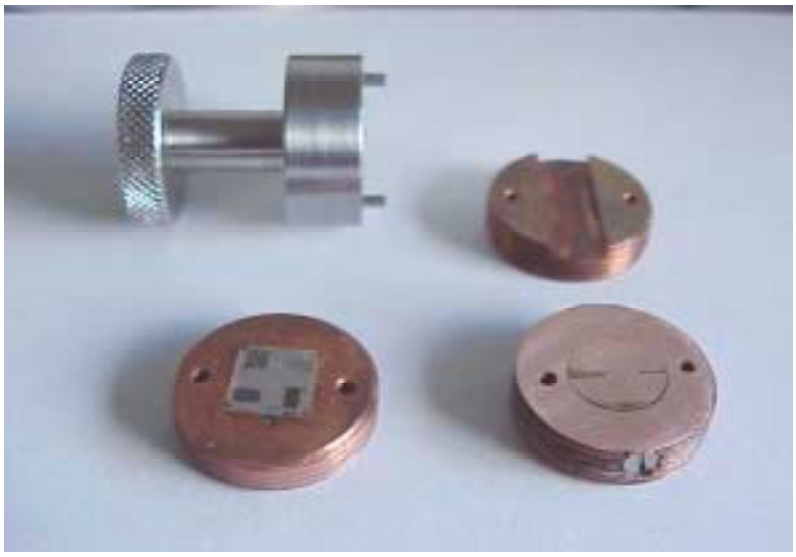

Figure B.2.1: Copper disc mounts for samples.

B.3 Magnetic coil and current supply

Several limiting factors exist in designing the coil. The maximum height that can fit between the table and the microscope is 110 mm. The coil must fit over the cryostat which requires an inner diameter of the bore-hole larger than 40 mm. The maximum diameter of the coil is 98 mm due to the microscope geometry. The maximum voltage over the coil should be limited to 50 V due to high voltage safety regulations. Within these constrictions we want to optimize the maximum obtainable magnetic field. An example of a calculation of this is shown in the mathcad file below:

Magnetic field at (x,y,z) from N*M turn coil with inner radius a and wire diameter d

$mm := 0.001 \cdot m \qquad \mu_0 := 4 \cdot \pi \cdot 10^{-7} \cdot \frac{henry}{m} \qquad \rho_{cu} := 1.68 \cdot 10^{-6} \cdot ohm \cdot cm$

coil dimensions

$innerradius := 23 \cdot mm$

$N := 25 \qquad n := 0 .. N - 1$ windings in radial direction

$d := 1 \cdot mm \qquad M := 100 \qquad m := 0 .. M - 1$ windings in vertical direction

$I := 4 \cdot amp$

$a(n, m) := innerradius + n \cdot d \qquad z_s(n, m) := \left(m - \frac{M}{2}\right) \cdot d$

$outerradius := innerradius + N \cdot d \qquad height := M \cdot d$

$height = 100 \cdot mm$

Analytical expression of field on central axis — z-axis has zero in the center of the coil

$$H_z(z) := 0.5 \cdot \frac{M \cdot N}{height} \cdot I \cdot \left[\frac{z \cdot mm + \frac{height}{2}}{\sqrt{\left(z \cdot mm + \frac{height}{2}\right)^2 + a\left(\frac{N}{2}, 0\right)^2}} + \frac{\frac{height}{2} - z \cdot mm}{\sqrt{\left(\frac{height}{2} - z \cdot mm\right)^2 + a\left(\frac{N}{2}, 0\right)^2}} \right]$$

$B_{zanalytic}(z) := \mu_0 \cdot H_z(z)$

Electrical properties

$$wirelength := \sum_m \sum_n 2 \cdot \pi \cdot a(n, m) \qquad wirelength = 0.55 \cdot km$$

$$R_{coil} := \rho_{cu} \cdot \frac{wirelength}{\left(\frac{\pi}{4} \cdot d^2\right)} \qquad R_{coil} = 11.76 \cdot ohm$$

$Power := I^2 \cdot R_{coil} \qquad Power = 188.16 \cdot watt \qquad turns := N \cdot M$

$Voltage := \frac{Power}{I}$

Results

$innerradius = 23 \cdot mm \qquad outerradius = 48 \cdot mm \qquad height = 100 \cdot mm \qquad turns = 2.5 \cdot 10^3$

$I = 4 \cdot amp \qquad Power = 188.16 \cdot watt \qquad Voltage = 47.04 \cdot volt$

$B_{zanalytic}(0) = 0.102 \cdot tesla \qquad B_{zanalytic}(25) = 0.093 \cdot tesla$

A coil with 2340 windings was wound on a brass reel. The reel has a borehole, which is 40mm in diameter, and the outer height is 108mm. The walls in the cylinder are 3mm thick and in the ends the walls are 4mm thick. The width of the reel is 110 mm. The coil was wound at the company:

VRT Transformer Aps
Mejeristræde 1
4000 Roskilde
phone: 46362197

for at prize of 2818 kr. They give the coil parameters to R = 12 Ohm and L = 81.3 mH at room temperature and the weight is 4.4 kg. The copper wire has a diameter of 1 mm.

Using a Gauss meter, the field in the center of the coil is determined to 492 G (0.049 T) at a fixed current of 2 A. This gives a conversion factor between current and magnetic field of 24.6 mT/A or 246 G/A.

A significant amount of power is dissipated in the coil at currents above 2A. In figure B3.1 the temperature of the coil is monitored as a function of time for different values of applied currents. The maximum current that should be applied to this coil is 5 A, but this should be used only in the automated macros, since this will minimize the time spent at this current. For 5 A the temperature of the coil will reach 80°C in less than 2 min. This gives a maximum field of 123 mT. The field should be independent of the temperature of the coil, since a constant current supply is used

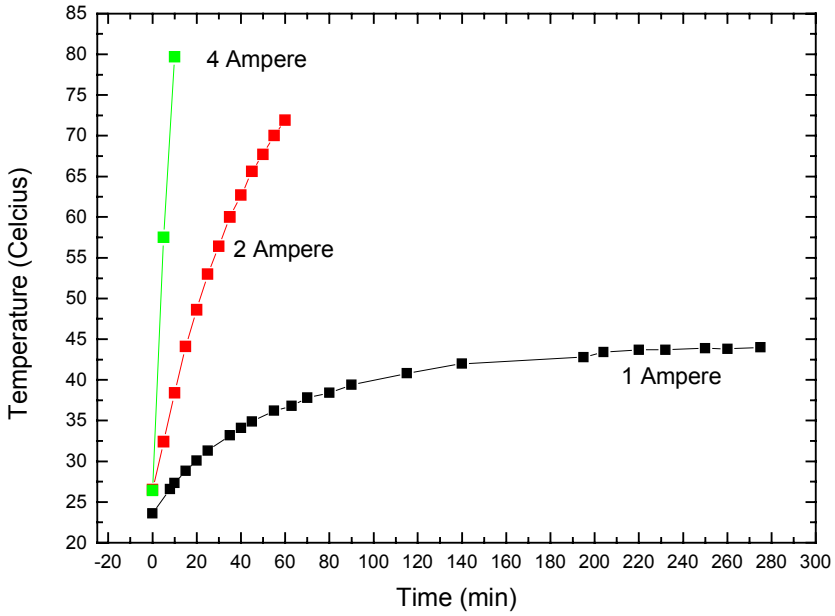

Figure B3.1: Temperature at the surface of the coil as a function of time for different currents.

The current supply is a Delta Electronics SM 70-22 with a maximum current output of 20A and a maximum voltage of 70V. It is connected to the measurement computer through a IEEE controller named PSC44M also from Delta Elecronics [19]. This controller has GPIB address 4. To change the current supply from remote mode to manual mode, two dip switches must be set on the back of the current supply. The current supply is seen in figure B3.2

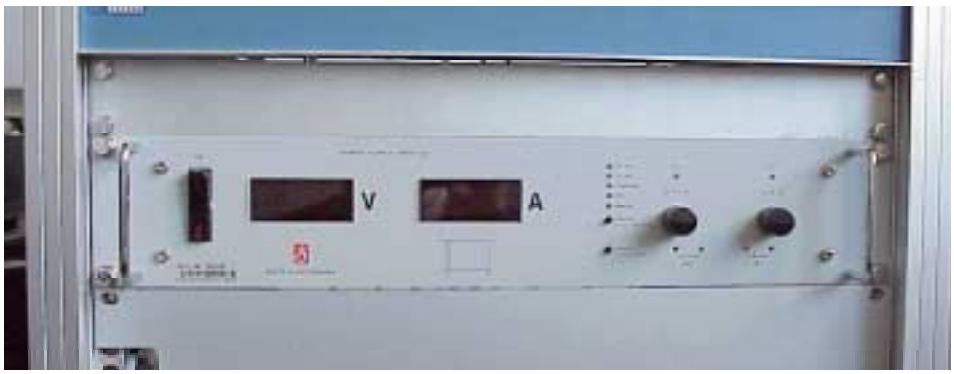

Figure B3.2: Current supply used to generate the external magnetic field

B.4 Image software and CCD camera

The images from the CCD is recorded using the program MTCi. The CCD camera and software has been purchased from

UNIT ONE electronics
Sandholmgårdsvej 38
3450 Allerød
phone: 4814 1670
contact person : Per Poulsen

The CCD camera is a SONY XC-75CE ½". It is black and white, has 768×576 pixels and 8 bits resolution. The computer is a 450MHz Pentium II with 786MB RAM and 10GB HDD. It has Windows NT with servicepack 3. The ethernet address on the netcard is 00105AF41C64

The program MTCi is found under C:\winnt\twain_32\mtci\mtci.exe. When a new user account is made under NT and the MTCi program is started, it starts in a demo version. To fix this one needs to choose 'help', 'about' and 'serial number'. In the menu, that appears the serial number: MTC2-11C8EC61-0D7D-5F1F is entered.

The driver for the framegrabber card is configured using the Oculus Tci configuration program. It is found under the 'start menu' under 'oculus'. In the configuration program 3 options appear. These are 'System VGA', 'Oculus Tci driver' and 'Bord 0 (Bus0 slot12). In the option 'Oculus Tci Driver' choose camera : generic CCIR/PAL. In the 'Bord 0 (Bus0 slot12)' option the following choices should be made: number of system memory frames: 232, min host: 0, width: 768, height: 576, monochrome 8bit, sync on composite video.

From UNIT ONE electronics we have purchased an extension to mTCI, which makes it possible to write commands to mTCI from a command line. This enables Tascom to communicate with mTCI. The extension was programmed by Marc Martin from UNIT ONE.

B.5 Microscope.

The microscope was purchased at:

DFA Dansk Fotoagentur A/S
Lersø Parkalle 101
DK2100 København Ø
phone: 3916 2020
fax: 3916 2040

It was brought piecewise. A list of the parts can be found in the MO binder in the laboratory. The microscope is mounted on a motorized stage.

Using a glass disc with a calibrated scale, the conversion factor between pixels in a picture and physical length is found. The conversion factor has been determined for 4 lenses with different magnification.

Lens magnification	conversion factor
× 2.5	7.20 µm/pixel
× 5	3.66 µm/pixel
× 10	1.87 µm/pixel
× 20	0.917 µm/pixel

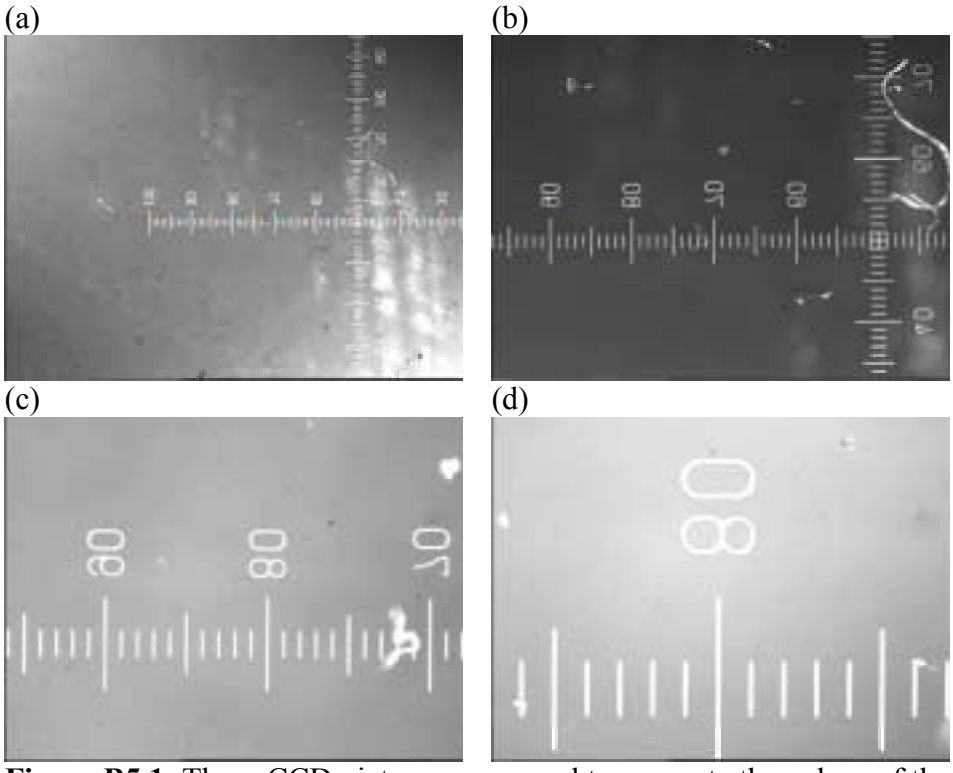

Figure B5.1: These CCD pictures were used to compute the values of the conversion factors. The magnification of the lenses were (a) ×2.5, (b) ×5, (c) ×10, (d) ×20. The total magnification of the microscope is not given by these numbers due to the ×0.45 lens in the 'neck'

B.6 MO films

Four magneto optical ferrite films were purchased from Russia. They are all 5x5x0.5mm. The substrate is Gadolinium-Gallium-Garnet and is 500 μm thick. The MO layer is Bismuth substituted ferrite garnet. The layer thickness vary as given below. The mirror layer is 0.3 μm Aluminum. The mirror layer is protected by a 0.1 μm Ti-TiN layer

The MO film thickness are : MO-3 : 5.7um
MO-4 : 2.1um
MO-13: 2.6um
MO-14: 6.5um

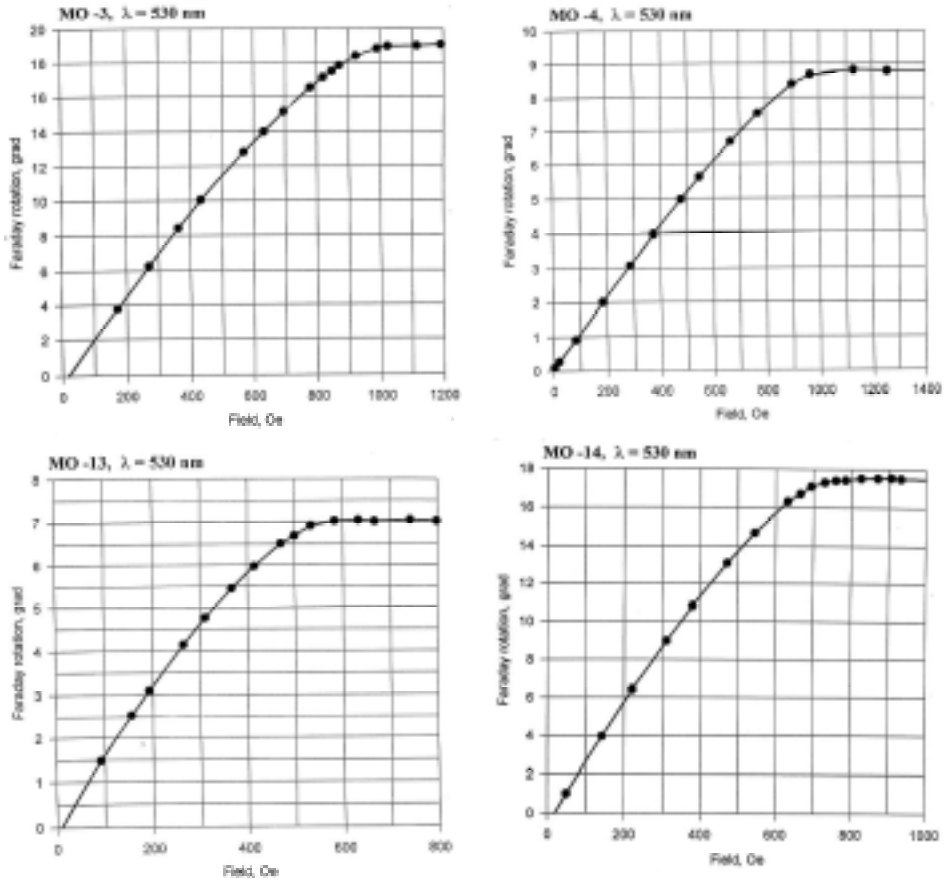

Figure B6.1: Field versus rotation angle for the 4 MO indicator films

Furthermore, some MO indicator films exists, which were obtained from Saarbrücken by M. Koblischka. The mirror layer on these is very fragile.

To clean the MO film M. Koblischka recommends [23] to use toluen followed by 2-5 minutes in ultrasound bath with an alcohol/acetone mixture. The MO indicator film may loose the important in-plane orientation if they are put under stress or the temperature is changed rapidly. The orientation can be reestablished by exposing the film to a large in-plane magnetic field. For the same reason, the MO indicator films should be stored with a large in-plane magnetic field, for instance in a box with permanent magnets attached.

B.7 Thermometers

The two thermometers mounted on the cold finger of the cryostat and under the sample disc respectively are calibrated DT-421-HR Lakeshore Silicon diodes [22]. The polarity of the diode is seen in figure B7.1(a). They were purchased at a prize of about 2800kr each through:

Aage Christensen A/S
Skelmosevej 10
postbox 399
2500 Valby
phone: 3644 2444
fax: 3677 2024

They were picked because of their small size and because they are non-magnetic. Their small size makes them very fragile, it is dangerously easy to tear one of the leads off. To protect the diodes and still ensure a good thermal contact to the cryostat, the diodes were mounted on a saphire plate following the procedure suggested by Lakeshore. A drawing of the mounting of the diode is shown in figure B7.1(b)
The serial number of the diodes are for the tip diode, T5: D37350T6 and for the sample diode: serial number D37349.

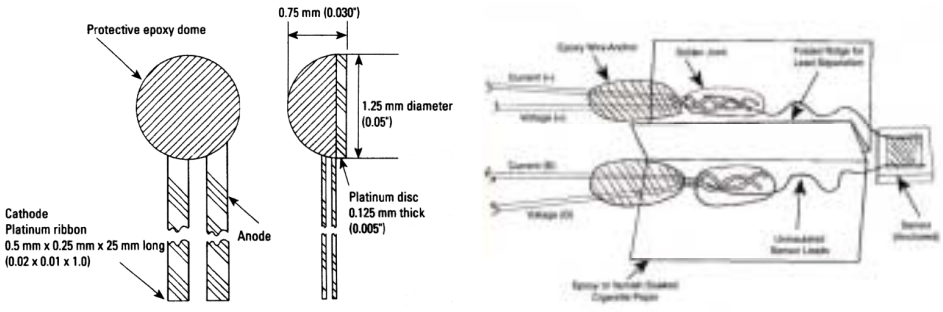

Figure B7.1: (a) Drawing of DT-420 diode showing the polarity. (b) Drawing showing how to safely mount the small diodes. From [22].

B.8 Temperature controller

Figure B8.1: Photograph of temperature controller with connections

The thermometers and the heater are controlled from a RISØ Digital temperature controller of type A1931a. A detailed description of all the features of this controller can be found in its manual [18]. The temperature controller has the GPIB address 8. The configuration of temperature controller is read by sending the command '?config' to the temperature controller (in tascom write tc'?config'). The result is:

```
CARD 0: VSBC-1 MC68000 SINGEL BOARD COMPUTER
CARD 1: P1926A DUAL PLATINUM THERMOMETER                1-2
CARD 2: P1928A DUAL THERMOCOUPLE THERMOMETER            3-4
CARD 3: P1929A DUAL DIODE THERMOMETER                   5-6
CARD 4: P1930A DUAL VOLTAGE OUTPUTS WITH MONITORS
CARD 5: P1906A ADSP2100 DIGITAL SIGNAL PROCESSOR
CARD 6: P2007A GPIB INTERFACE
```

In figure B8.1 the temperature controller with the installed modules is seen. Starting from left is the VSBC-1 single board computer, which also has the connector to the monitor. Between the two connectors seen are two small buttons. The smaller left one is used to reset the memory of the controller by clearing the thermometer calibration tables, the PID parameters etc. The next module is the digital signal processor P1906a and then the P2007a GPIB interface. Next follows the 3 temperature modules. The platinum and thermocouple modules are not used. The two Silicon diodes are connected to the P1929a module. Due to the position of the Diode module they are named temp5 (sample thermometer) and temp6 (finger thermometer). The P1930 voltage output sends a voltage proportional to the wanted heater output out. This is amplified by the large module to the far right in the photograph. This is a 0-50V/1A power supply.

The output voltage from module P1930a is calculated by the processor using the temperature calibration tables and the PID tables which is read into the temperature controller when it is initialized. The Tascom file to initialize temperature system is seen below:

moinit.tas:

```
!*****************************************************
!** MOINIT6 THE TEMPERATURE CONTROLLER for the MO system
!** 3rd version 9.10.2000
!** 2 diode thermometers in tip and finger on output 5 and
6
!** finger diode controls output of max 36V to tipheater
!**
!*****************************************************
TFIL=37349    ! calibrated diode in tip - channel 5
TFIL=37350    ! calibrated diode in finger - channel 6
CFIL=990831   ! PID file He, 5psi, 50/50mm flow
TC'OUT1=VCCO6'
TC'MON=1,TEMP5,vcco6,TEMP6'
```

The lines starting with '!' are comments. The first line assigns the calibration table t37349 found in c:\tascom\tassup2\command\tfil to the thermometer in channel 5. The t37349.tas files has the following structure:

```
CAL6="MO finger temp DT421-HR serial D37349. 9.10.2000 bhl"
UNIT: "K"
1.20071123189472, 1.85136
1.30632803880896, 1.85037
1.40225623329815, 1.84936
...
320.137262265882, 0.473006
326.054385346976, 0.459281
329.980489861145, 0.450216
END
$END
```

The next line assigns the thermometer in channel 6 to the calibration table t37350.tas. The third line in the initialization file gives the file where the PID parameters for the system are given as a function of temperature. The file c990831.tas is located in c:\tascom\tassup2\command\cfil and has the following structure:

```
PID6 = "MOSETUP 31.8.1999 BHL He cool, 50/50mm 5psi"
PARM: 0.3, 5.0, 0.000000E00 , 0.0, 60.0
  20.000,  2.015196E-01,   0.000,    1.640,    0.410,   0.0, 60.0
  25.000,  2.093529E-01,   0.000,    3.298,    0.825,   0.0, 60.0
...
  85.000,  2.734294E-01,   0.000,    9.854,    2.464,   0.0, 60.0
  90.000,  3.082035E-01,   0.000,    8.894,    2.224,   0.0, 60.0
END
$END
```

The fourth line assigns the thermometer in position 6 give the output that controls the heater using the PID parameters given. Thermometer 6 is mounted on the cold finger below the entire sample mount. The last line determines which variables to write to the monitor.

The electrical connections to the cryostat consist of cables to the thermometers and to the heater. The cryostat heater is a 36 V, 36 W coil wound at the end of the cold finger. It is mounted from the factory. Four

wires in white shrouds are wound around the finger from the factory and are used for the heater. They connect to the 6-pol Ceramaseal connector. 12 additionally 0.15 mmØ copper wire has been wound around the cold finger. They connect to a 10-pin Lemo connector on the cryostat. The two thermometers are connected to this connector.

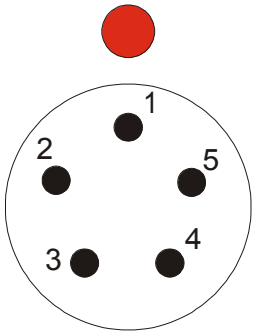

Figure B8.2(a) The 5-pin Lemo male connector seen from outside

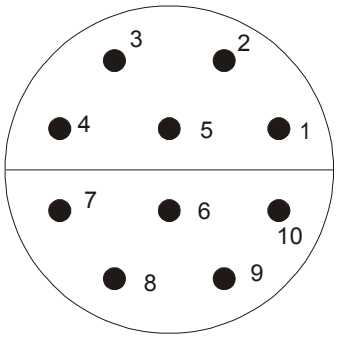

Figure B8.2(b) The 10-pin Lemo connector on the cable from the temperature controller plugged into the cryostat

The table below shows how the two 5-pin Lemo connectors from the temperature controller are connected to the 10 pin Lemo connector on the cryostat. The pin numbers are given in figure B8.2.

5-Lemo's	Wire color	10-Lemo	Si-diodes
tip-ch5-1	White	1	37349-anode(+)
tip-ch5-2	Brown	2	37349-anode
tip-ch5-3	green	3	37349-cathode(-)
tip-ch5-4	Yellow	4	37349-cathode
finger-ch6-1	Brown	7	37350-anode
finger-ch6-2	Yellow	8	37350-anode
finger-ch6-3	Green	9	37350-cathode
finger-ch6-4	Grey	10	37350-cathode

In Tascom to start tip heater write:

```
tascom> tc'set6=300'
tascom> tc'vcc6=on'
```

To stop tip heater:

```
tascom> tc'vcc6=off'
```

Do not use tip heater without Helium cooling since this may burn the heater.

B.9 TASCOM

Tascom is a command program originally designed to control a triple axis spectrometer [18]. It controls the communication to instruments and has a programming language, which can either be used as command line input or in command files. For the magneto optical system a customized version of Tascom was made by Per Skaarup. The program communicates over the IEEE bus with the temperature controller and the magnetic coil current supply. Furthermore, it sends commands to the mTCI image program using an extension to the mTCI program.
The Tascom version used is c:\tascom\tassup2\tascomsu.exe. The temperature calibration tables and the PID parameter lists are in c:\tascom\tassup2\command\tfil and c:\tascom\tassup2\command\cfil. The default location for command files is c:\tascom\tassup2\command\mycom. But using the command 'com_dir=' command files from other locations can be executed.

Below is a list of useful Tascom commands:

moinit5	Initializes the temperature controller
data_dir ='dirname'	Data are saved in d:\data\dirname
com_dir='dirname'	command files and batch files are run from c:\tascom\sup2\command\dirname (default is ..\command)
fina='fname'	part of name of datafile, max 6 characters
segn=0	The full name of datafile is fname + segn
seccd=0	The full name of a picture is fname + seccd
dfit='description'	text in each data file

A command string is sent to the temperature controller using the TASCOM command tc' '. Temp5 is the sample thermometer, temp6 is the finger thermometer (controlling)

tc'set6=120'	set the setpoint of thermometer 6 to 120K
tc'vcc6=on' (or =off')	enable the feedback loop to the heater
tc'?temp5'	query the value of thermometer 5
tc'?status'	show setup of the temperature controller

Drivers from tascom interfacing with the image program MTCi:

snap	takes a picture (.tif) and keeps it in buffer.
grab	show live picture on screen
ccd_save	saves the picure in the buffer to fname+seccd.tif

A command string it sent to the coil current supply using the TASCOM command psc44' '. The current supply has 12 bit resolution :

psc44'fu70,fi20'	initializes the current supply to full scale 70V, 20A
psc44'i',3	set the current to 3A (initialization must preceed this)
psc44'SA4096,SB0'	set to full scale in voltage equal 12 bit
psc44'MB?'	read back the voltage in number of steps out of 12 bit

In the following are 3 examples of command files:

```
!*****************************************************
!** templine.TAS
!** Britt Hvolbæk Larsen, Risoe, 8.10.1999
!** Tascom command file to log the temperatures for the
!** tip and finger
!**
!*****************************************************
var:timeinterval                    !scan variables
?' log t5 and t6 vs time'
reap
segn=segn+1
t0=time
localtime=time
power=0
afip localtime, temp5, temp6        !variables to file
aprp localtime, temp5, temp6        !variables to screen
WHLE step.le.endstep
    wait timeinterval
    localtime=time-t0
   ! power=tc'?vcco6'
    out
NEXT
dplo localtime,temp5
plot
reap


!*****************************************************
!** magloop.TAS
!** Britt Hvolbæk Larsen, Ris>, 24.1.2000
!** extends mramp1 by including ccd_save
!** Tascom command file to ramp magnetic field up and down
!** while taking a picture at each field (or just pausing.
!**
!*****************************************************
var:bbeg,bend,db                    !scan variables
?' scan with current in PSC44/delta electronic current sup-
ply'
reap
segn=segn+1
psc44'fu70,fi20'
! ***** convert current to steps - more precise than direct
current
begstep=ABS(bbeg*4096/20)
endstep=ABS(bend*4096/20)
dstep=ABS(db*4096/20)
! ***** end convert
b=bbeg
step=begstep
curr=-1
volt=-1
psc44'sa4096,sb0'
afip step, curr, volt, seccd, temp5, temp6      !variables
to file
aprp step, curr, volt, seccd, temp5, temp6      !variables
to screen
dplo curr,volt
WHLE step.le.endstep
```

```
  psc44'SB',step
  wait 1
  psc44'MB?'
  curr=vdig*20/4096
  psc44'MA?'
  volt=vdig*70/4096
  wait 1
  seccd=seccd+1
  snap
  ccd_save
  out
  step=step+dstep
NEXT
rampdown=1
! ASK_VAR'rampdown? yes=1',rampdown
IF rampdown.EQ.1
  step=step-2*dstep
 WHLE step.gt.begstep
  psc44'SB',step
  wait 1
  psc44'MB?'
  curr=vdig*20/4096
  psc44'MA?'
  volt=vdig*70/4096
  seccd=seccd+1
  snap
  ccd_save
  out
  step=step-dstep
  NEXT
END
psc44'sa4096,sb0'
plot
reap


!*****************************************************
!** snap2file.TAS
!** Britt Hvolb'k Larsen, Asger Abrahamsen, Risoe, 2.2.2001
!** Tascom command file to take pictures and save settings
to
!** log files
!**
!*****************************************************
?' save picture t5 and t6'
reap
segn=segn+1
t0=time
picture=0
settemp=0
localtime=time
psc44'fu70,fi20'
tc'vcc6=on'
afip localtime, temp5, temp6        !variables to file
aprp localtime, temp5, temp6        !variables to screen
en=1
to=2
WHLE en.le.to                       !infinite loop
ASK_VAR'enter new set temperature',settemp
tc'set6=',settemp
!vent på tegn fra bruger
```

```
ASK_VAR'take picture? yes=1',picture
  IF picture.EQ.1
   !tag billede
   seccd=seccd+1
   snap
   !gem billede
   ccd_save
   !læse strøm
   psc44'MB?'
   curr=vdig*20/4096
   psc44'MA?'
   volt=vdig*70/4096
   localtime=time-t0
   !til datafil : billedenavn, t5, t6, current, voltage,
localtime
   afip seccd, temp5, temp6, curr, volt, localtime
   aprp seccd, temp5, temp6, curr, volt, localtime
   dplo localtime,temp5
   out
  END       !take picture IF
NEXT
reap
```

B.10 _Petriina Paturi's Scilab program

On the basis of the paper by Wijngaarden *et al*. [11], Petriina Paturi of the University of Turku, Finland has made a program that calculates the current density from a picture of the intensity from the MO film and a mathematical expression of how to convert the intensity into magnetic field strength. Petriina can be reached at:


```
Petriina Paturi                      tel.   +358-2-333 5676
Wihuri Physical Laboratory           fax.   +358-2-231 98
Department of Physics
FIN-20014 University of Turku        e-mail peetu@utu.fi
Finland
```


The program 'wijn_n' is run from Scilab, which is a Matlab-like program for Linux. Scilab is available on fys-lin-2. Besides Scilab, a packet with tiff-applications must be installed. The program uses several routines that have been programmed in C in order to speed up the calculation time. The following files are needed for a simulation:

wijn_n.sci	The main program
wijnbatch.sci	The main program in a version that uses an input file and not clicks on menus
wijn_func.sci	different functions used by wijn_n.sci
gsolve_u.c	matrix inversion written in C
tiff2sci.c	Converts .tif files to files for Scilab
nrutil.c and nrutil.h	
toeplz.c	

The gsolve_u.c and tiff2sci.c should be compiled by writing:

```
gcc -o gsolve_u gsolve_u.c -lm
```

This uses the nrutils.c and toeplz.c files. The use of the wijn_n program is described in details in the user guide for image processing in appendix A.2. A version of this program, which uses a text file for input parameter instead of entering the input data by hand, is called wijnbatch.sci. Note that the length scale for film thickness and distance between sample and indicator film should be given in pixels. Knowing the physical distance and the magnification of the microscope (see appendix B.5) the distances in pixels can be determined. The length scales must be given in pixels for numerical reasons. This also makes the program microscope independent.

To obtain a good current inversion it is necessary to make a background correction to the image with the data. The background correction eliminates any uneven light distribution from the microscope. It also corrects for local defects in the MO indicator (holes) and scratches. It is therefore imperative for good data acquisition that background pictures are taken

with no sample (i.e. above T_c) and the MO indicator and polarizers are in the same position as the data image.
To correct the data image, first the bias of the CCD camera must be substracted. This is the intensity seen in a picture with zero applied magnetic field and it stems from the bias of the CCD chip and the deviation from 90° between the polarizers. This intensity must be substracted from both the data image and the background image.
The assumption of the correction is that the signal at defects is darker than the surrounding indicator film by a proportional factor. This means that if the data image is normalized to the background image, the defects will be 'amplified' to the level that could be expected if there was no defect. The normalization also flattens any uneven light distribution. So the background correction consists of taking the data image and background image at the same magnetic field, making sure the positions of the defects overlap and then dividing the data image with a normalized background image (normalized to its own average). By dividing with a normalized image the absolute value of the intensity of the data image is preserved. This value can be directly related to the field strength. The alignment of the two images and the division and normalization is done using the ImagePro program.
The absolute value of the intensity of the field strength is important for the inversion to a current density map. The dependence of the intensity of the images from the MO microscope and the field strength is determined also from the background images, which again stresses the importance of having these. With no sample (or above T_c) the applied field is swept and pictures at several values are taken. Ideally, these should show a uniform intensity. By plotting the average intensity against the applied magnetic field the functional dependency of magnetic field strength and pixel intensity can be found. The deviation from uniform intensity in the background pictures can be used to clean up the data picture, as described above. See also chapter 3.2. The area picked for calculating the current density must be quadratic.

A list of useful Scilab commands:

exec('wijn_n.sci')	runs the wijn _n.sci program
size(J)	shows the dimension of the J matrix
T=J(10:90,10:90)	makes a new matrix T from the elements of row 10-90, column 10-90
J=read('filename',N,M)	reads a NxM matrix from the file called filename
contour(1:N,1:M,matrix,no-of-contours)	make contour plot
grayplot(1:N,1:M,matrix)	make matrix plot
xbasc()	clear plot window

The structure of a batch file shown below:

```
filename="/home/fys/brhl/wijngaarden/data/ipttomorapp/B55r0066cor.tif"
savename="/home/fys/brhl/wijngaarden/data/ipttomorapp/B55r0066a"
startX=    10
startY=    100
N=         550
```

```
HvsI=      "62.8*asin((x-130.7)/125.8)+109.7"
thickness= 1
distance=  1
// next line is either "before", "after" or "none"
filter= "none"
filter_r=  7
```

Not that to get the current density in units of A/m^2 the J matrices must be multiplied with:

$$\frac{10^{-3}}{4\pi \cdot 10^{-7} \cdot pixellength}$$

where *pixellength* is the size of the pixels in meters.

Example of data analysis:

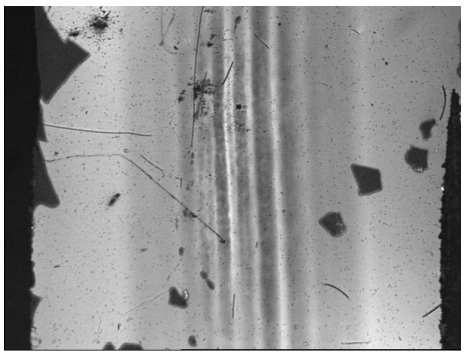

001026/B55r0066bw.tif.5A, 23mT, 7K, IPT, 55 filaments, rolled from round

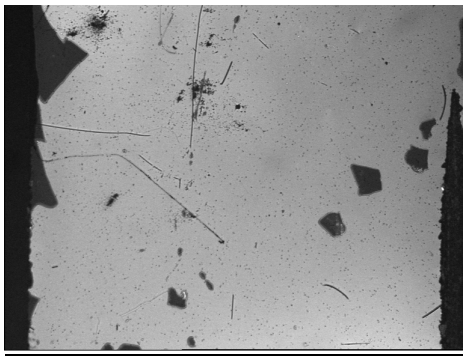

001026/B55r0056bw.tif,5A, 123mT, 105K for background correction

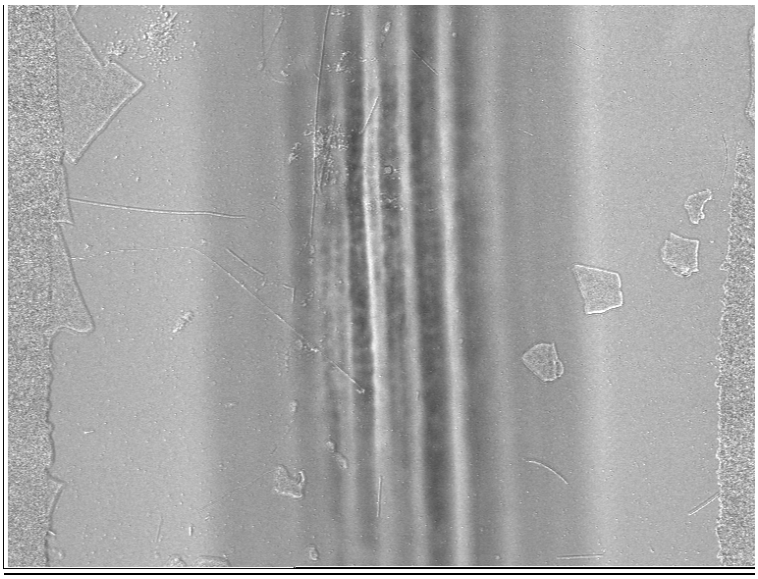

The corrected image

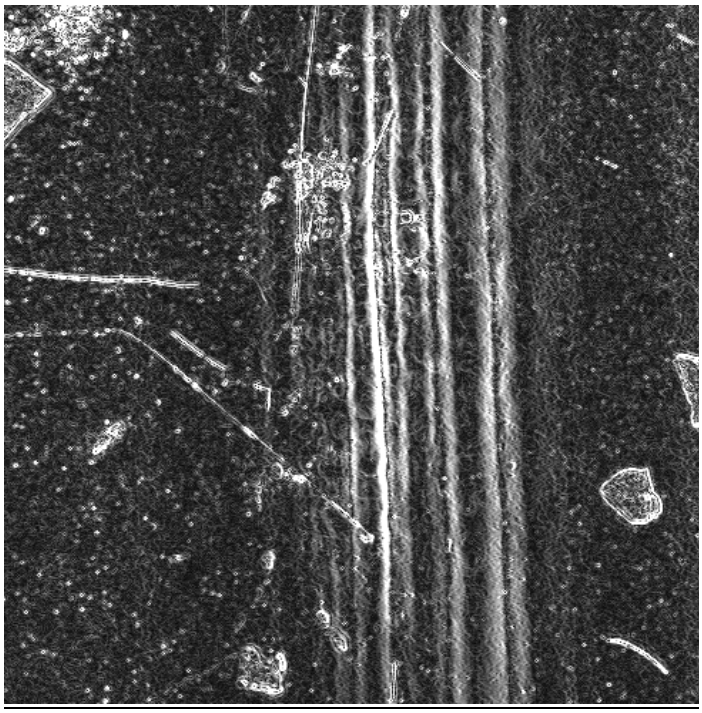

The current density image

A few examples of scilab files are shown below:

showjc.sci:

```
name='B55r0066a';
N=550;
jj=read('/home/fys/brhl/wijngaarden/data/ipttomorapp/'+name+'.j',N,N);
jreal=jj*1e-3/(4*%pi*1e-7*3.57e-6);
ud='rm '+name+'.jreal';
unix(ud);
write(name+'.jreal',jreal);
s=jreal(10:N-10,N/2);
t=plot2d(s);
```

showaverage.sci:

```
xbasc();
name='B55r0066a';
N=550;
jj=read('/home/fys/brhl/wijngaarden/data/ipttomorapp/'+name+'.jx',N,N);
jreal=jj*1e-3/(4*%pi*1e-7*3.57e-6);
ud='rm '+'/home/fys/brhl/wijngaarden/data/ipttomorapp/'+name+'.jxreal';
unix(ud);
write('/home/fys/brhl/wijngaarden/data/ipttomorapp/'+name+'.jxreal',jreal
);
stemp=0;
for i=20:N-20,;
  stemp=stemp+jreal(i,10:N-10);
end;
s=stemp/(N-59);
//s=jreal(10:N-10,N/2)
t=plot2d(s);
ud='rm '+'/home/fys/brhl/wijngaarden/data/ipttomorapp/'+name+'.jxprofil';
unix(ud);
write('/home/fys/brhl/wijngaarden/data/ipttomorapp/'+name+'.jxprofil',s);
```

B.11 Polishing samples

The following is based on M. Koblischka's report on the MO technique [23] which should be consulted for further details.

Polishing is used e.g. for high-resolution imaging of superconducting tapes. In normal cases, it is sufficient to polish the top layer of the sample, without reaching the superconducting core of the tape. This should be done slowly with 2400-paper, in order to detect when the superconductor is reached.
If a high-resolution is required, a full polishing where part of the filaments is removed can be considered. A full polishing procedure consists of grinding with grinding papers 800, 1000, 1200, 2400, and 4000, followed by a polishing step (on the special STRUERS cloth) using the OP-S suspension. Each polishing step should be of about 2 to 5 min. in duration; longer times are recommended for the 2400 and 4000 paper. It is recommended to use dry polishing and only use ethanol when cleaning is needed between the steps. The final polishing step with the OP-S suspension should be about 10 min. long. The OP-S suspension is a trademark from Struers A/S, and it consists of a colloidal suspension of oxide particles with a grain size of approx. 0.1 μm. This suspension does not damage the superconducting properties of the tape samples (and most other superconducting materials). The often used Diamond paste contains too many organic solvents, which may enter into the superconductor and spoil the superconducting properties. An easier way is to remove the top Ag-layer by chemical etching [23]

B.12 Improvements and tests to be done

- A test should be performed to determine the temperature difference between the sample on top of the sample disc and the sample thermometer situated below the sample disc in the sample mount. A way to do this would be to unmount the cold finger thermometer and place it at the sample position.
- The mTCI software can record time sequences. This ability should be explored
- repair potentiometer on CCD for manual gain
- Make several MO images on multifilament tape with polishing in between images to give 3D field distribution.

C. LITERATURE

[1] M. R. Koblischka and R. J. Wijngaarden.
Magneto-optical investigations of superconductors .
Supercond. Sci Technol. **8** (1995) 199-213.

[2] T. H. Johansen *et al.*
http://www.fys.uio.no/faststoff/ltl/

[3] T. H. Johansen *et al.*
Presented at the APS meeting in Seattle 2001
privat communication.

[4] P. Paturi
Laser ablation of superconducting YBCO films from nonopowder target and preparation of mesoscopic YBCO/Au interfaces
Ph. D. Thesis, University of Turku (1998)

[5] T. Frello
Structural and superconducting properties of high-Tc superconductors
Ph. D. Thesis(1999), RISØ-R-1086, ISBN 87-550-2476(EN)

[6] E. Zeldov, J. R. Clem, M. McElfresh and M. Darwin
Magnetization and transport currents in thin superconducting films
Phys. Rev. B. **14** (1994) 9802-9822.

[6] E. H. Brandt
Superconductor disks and cylinders in an axial magnetic field
Phys. Rev. B. **55** (1998) 6506-6522

[8] E. H. Brandt
The flux-line lattice in superconductors
Rep. Prog. Phys. **58** (1995) 1465-1594.

[9] C. Joos, R, Warthmann, A. Forkl, H. Kronmüller
High-resolution magneto-optical imaging of critical currents in $YBa_2Cu_3O_{7-\delta}$ thin films.
Physica C **299** (1998) 215-230.

[10] S. Chatraphorn, E. F. Fleet, F. C. Wellstood, L. A. Knauss, T. M. Eiles
Scanning SQUID microscopy of integrated circuits
App. Phys. Lett. **76** (2000) 2304-2306.

[11] R. J. Wijngaarden, H. J. W. Spoelder, R. Surdeanu and R, Griessen.
Determination of two-dimensional current patterns in flat superconductors form magneto-optical measurements : An efficient inversion scheme.
Rhys. Rev B, **54** (1996) 6742-6747.

[12] M. Baziljevich, T. H. Johansen, Y. Galperin, P. E. Lindelof, Y. Shen and P. Vase.
New simple method to measure j_c in superconducting films using magneto-optics.
Physica C **266** (1996) 127-132

[13] T. H. Johansen, M. Bazilejvich, H. Bratsberg, Y, Galperin, P. E. Lindelof, Y. Shen and P. Vase.
Direct observation of the current distribution in thin superconducting strips using magneto-optic imaging.
Phys. Rev. B **54** (1996) 16264-16269

[14] R. J. Wijngaarden, K. Heeck, H. J. W. Spoelder, R. Surdeanu, R. Griessen.
Fast determination of 2D current patterns in flat conductors from measurements of their magnetic field.
Physica C **295** (1998) 177-185

[15] E. H. Brandt and M. Indenbom
Type-II-superconductor strip with current in a perpendicular magnetic field
Phys. Rev B **48** (1993) 12893-12906

[16] APD Air Products and Chemicals Inc
Model LT-3-110 heli-tran liquid transfer refrigeration system
1994

[17] Engineering and Computer Department
A1931A Digital Temperature Controller, User's manual
RISØ-I-756(EN) (1994)

[18] J. Bundgaard, K. Enevoldsen and R. Skaarup
Tascom user manual
Risø 1995

[19] Delta Elektronika BV
PSC 44M Power supply controller manual and SM 70-22 manual

[20] M. R. Koblischka, T. H. Johansen, B. H. Larsen, N. H. Andersen, H. Wu, P. Skov-Hansen, M. Bentzon and P. Vase
Magneto-optical investigation of multifilamentary Bi-2223 tapes
Physica C **341-348** (2000) 2583-2584.

[21] H. Sørensen, B. Sass and K.V.Weisberg
Note on Si Diode Thermometers
RISØ-I-551

[22] Lakeshore
Temperature Measurement and Control catalog

[23] M. Koblischka
MO for beginners
NST report (2001)

Bibliographic Data Sheet **Risø-R-1262(EN)**

Title and authors

The Magneto Optical System at Risø

Britt Hvolbæk Larsen

ISBN 87-550-2867-5

ISSN 0106-2840

Department or group: Materials Research Department

Date: April 2001

Groups own reg. number(s)

Project/contract No(s)

Sponsorship

Statens Teknisk Videnskabelige forskningsråd (STVF),
Energistyrelsen (EFP)

Pages	Tables	Illustrations	References
70	5	38	23

Abstract (max. 2000 characters)

The new magneto optical system at Risø is presented in details. Results measured on the system is shown. Image correction and magnetic field to current density conversion is described.

Descriptors INIS/EDB

Available on request from Information Service Department, Risø National Laboratory,
(Afdelingen for Informationsservice, Forskningscenter Risø), P.O.Box 49, DK-4000 Roskilde, Denmark.
Telephone +45 4677 4004, Telefax +45 4677 4013, email: risoe@risoe.dk